NASA/TM—2005-213988 AIAA–2005–5671

Off-Nominal Performance of the International Space Station Solar Array Wings Under Orbital Eclipse Lighting Scenarios

Thomas W. Kerslake
Glenn Research Center, Cleveland, Ohio

David A. Scheiman
Ohio Aerospace Institute, Brook Park, Ohio

October 2005

The NASA STI Program Office . . . in Profile

Since its founding, NASA has been dedicated to the advancement of aeronautics and space science. The NASA Scientific and Technical Information (STI) Program Office plays a key part in helping NASA maintain this important role.

The NASA STI Program Office is operated by Langley Research Center, the Lead Center for NASA's scientific and technical information. The NASA STI Program Office provides access to the NASA STI Database, the largest collection of aeronautical and space science STI in the world. The Program Office is also NASA's institutional mechanism for disseminating the results of its research and development activities. These results are published by NASA in the NASA STI Report Series, which includes the following report types:

- TECHNICAL PUBLICATION. Reports of completed research or a major significant phase of research that present the results of NASA programs and include extensive data or theoretical analysis. Includes compilations of significant scientific and technical data and information deemed to be of continuing reference value. NASA's counterpart of peer-reviewed formal professional papers but has less stringent limitations on manuscript length and extent of graphic presentations.

- TECHNICAL MEMORANDUM. Scientific and technical findings that are preliminary or of specialized interest, e.g., quick release reports, working papers, and bibliographies that contain minimal annotation. Does not contain extensive analysis.

- CONTRACTOR REPORT. Scientific and technical findings by NASA-sponsored contractors and grantees.

- CONFERENCE PUBLICATION. Collected papers from scientific and technical conferences, symposia, seminars, or other meetings sponsored or cosponsored by NASA.

- SPECIAL PUBLICATION. Scientific, technical, or historical information from NASA programs, projects, and missions, often concerned with subjects having substantial public interest.

- TECHNICAL TRANSLATION. English-language translations of foreign scientific and technical material pertinent to NASA's mission.

Specialized services that complement the STI Program Office's diverse offerings include creating custom thesauri, building customized databases, organizing and publishing research results . . . even providing videos.

For more information about the NASA STI Program Office, see the following:

- Access the NASA STI Program Home Page at ***http://www.sti.nasa.gov***

- E-mail your question via the Internet to help@sti.nasa.gov

- Fax your question to the NASA Access Help Desk at 301–621–0134

- Telephone the NASA Access Help Desk at 301–621–0390

- Write to:
  NASA Access Help Desk
  NASA Center for AeroSpace Information
  7121 Standard Drive
  Hanover, MD 21076

NASA/TM—2005-213988 AIAA–2005–5671

Off-Nominal Performance of the International Space Station Solar Array Wings Under Orbital Eclipse Lighting Scenarios

Thomas W. Kerslake
Glenn Research Center, Cleveland, Ohio

David A. Scheiman
Ohio Aerospace Institute, Brook Park, Ohio

Prepared for the
Third International Energy Conversion Engineering Conference
sponsored by the American Institute of Aeronautics and Astronautics
San Francisco, California, August 15–18, 2005

National Aeronautics and
Space Administration

Glenn Research Center

October 2005

Acknowledgments

The authors would like to acknowledge and sincerely thank the following individuals for their help: David Karakula and David Moore, The Boeing Company, for providing ISS artificial lighting information relevant to CETA lamps, VCLs and EMU helmet lights; Andre Tolbert and, David Karakula, Boeing; and Nate Jones, NASA Kennedy Space Center, for processing the Avionics Equipment Request to the ISS Avionics Equipment Panel to allow NASA Glenn Research Center, to borrow the qualification VCL unit located at NASA Kennedy in support of this test program; and Ann Delleur, Julia Holda (intern) and Eric Gustafson (co-op) of NASA Glenn, for their gracious and valuable assistance in conducting the PPM panel testing with the VCL light source.

This report contains preliminary findings, subject to revision as analysis proceeds.

Available from

NASA Center for Aerospace Information
7121 Standard Drive
Hanover, MD 21076

National Technical Information Service
5285 Port Royal Road
Springfield, VA 22100

Available electronically at http://gltrs.grc.nasa.gov

Contents

Executive Summary

This report documents test activities, data and analyses to quantify International Space Station (ISS) solar array wing (SAW) string electrical performance under highly off-nominal, low-temperature-low-intensity (LILT) operating conditions with non-solar light sources. This work is relevant for assessing feasibility and risks associated with a revised Sequential Shunt Unit (SSU) remove and replace Extravehicular Activity (EVA).

Based on this assessment of worst-case (greatest) SAW string steady state electrical performance under best-case (greatest) eclipse lighting conditions, there is no connector pin molten metal hazard. There is no EVA crew member shock hazard for cases of full moon illumination or Extravehicular Mobility Unit (EMU) helmet lighting conditions or combined full moon plus EMU helmet lighting conditions. However, EVA crew member electrical current and/or voltage hazards limits were exceeded for certain Video Camera Luminaire (VCL) lighting cases. Operational solutions to mitigate SAW string electrical hazards from VCL illumination include: (1) power down the VCL at issue or (2) select a VCL pan angle to point the beam away from the SAW.

Based on additional analysis, there is minimal risk of electrostatic discharge from or between SAW string solar cells under any eclipse lighting condition. Similarly, there is minimal risk of electrostatic discharge at SSU power connectors and test port connectors due to steady state SAW string current and voltage under any eclipse lighting condition.

The authors recommend that the SAW string electrical performance assessment under VCL eclipse lighting conditions be repeated once detailed and accurate SSU remove & replace EVA procedures have been developed. The product of this assessment would be SAW gimbal and/or VCL pan angle keep-out-zones (KOZs) to decrease SAW current and voltage levels generated as a result of VCL lighting to safe levels. The authors also recommend that the EVA crew member electrical hazard thresholds be confirmed as-is or revised to the best possible values to maximize crew safety. The uncertainty level in this proposed detailed KOZ assessment could be reduced with additional VCL lighting data.

Off-Nominal Performance of the International Space Station Solar Array Wings Under Orbital Eclipse Lighting Scenarios

Thomas W. Kerslake
National Aeronautics and Space Administration
Glenn Research Center
Cleveland, Ohio 44135

David A. Scheiman
Ohio Aerospace Institute
Brook Park, Ohio 44142

Abstract

This paper documents test activities, data and analyses to quantify International Space Station (ISS) Solar Array Wing (SAW) string electrical performance under highly off-nominal, low-temperature-low-intensity (LILT) operating conditions with non-solar light sources. This work is relevant for assessing feasibility and risks associated with a Sequential Shunt Unit (SSU) remove and replace (R&R) Extravehicular Activity (EVA). The SSU is an electronics box that regulates the primary power system bus voltage by matching the SAW current output to the channel load demand. It is desirable to conduct the SSU R&R EVA without retracting the SAW. With the SAW deployed, there is an electrical risk of mating/demating SAW input connectors to the SSU. Even during orbital eclipse EVA operations, SAW strings can be energized by low-intensity, non-solar, natural light sources, such as the moon, and artificial light sources, such as EVA suit helmet lights or video camera lights. To quantify SAW electrical performance under this off-nominal, non-solar, low-temperature, low-intensity (LILT) illumination, solar cell and solar cell panel electrical performance testing was performed using full moon, solar simulator and Video Camera Luminaire (VCL) light sources. Laboratory test conditions included temperatures from ambient to –110 °C and illumination intensities from 1-Sun to 0.0001-Suns. Terrestrial full moon testing was conducted under typical ambient conditions of the north eastern Ohio in the late spring. An eclipse orbital lighting assessment was also performed to quantify the maximum lighting intensities on the SAW from all credible natural and artificial sources. By combining the measured steady state electrical performance data and the calculated orbital eclipse lighting intensity, SAW string current and voltage performance levels were calculated and compared with established electrical hazard thresholds. The results of this comparison for all credible light sources are presented in the paper. These results are discussed in the context of crew member shock hazards and connector pin molten metal hazard. Results, uncertainties and limitations are also discussed along with operational solutions to mitigate potential SAW string electrical hazards from VCL illumination. Finally, results from a preliminary assessment of SAW arcing to the space plasma or within power connector pins are discussed. The authors recommend that the SAW string electrical performance assessment under VCL eclipse lighting conditions be repeated and expanded once detailed and accurate SSU R&R EVA procedures have been developed. The product of this assessment would be SAW gimbal and/or VCL pan angle keep-out-zones (KOZs) to decrease SAW current and voltage levels generated as a result of VCL lighting to safe levels.

1.0 Background

The Sequential Shunt Unit (SSU) is an electronics box that regulates the International Space Station (ISS) primary power system bus voltage by matching the US Solar Array Wing (SAW) current output to the channel load demand. There is one SSU per SAW and at assembly complete, the ISS will have eight active SSUs. The baseline SSU removal and replacement (R&R) Extravehicular Activity (EVA) calls for the SAW to be fully retracted. This places the solar array blankets into compact fan-folded, panel stacks with minimal light reaching solar cells. In this configuration, solar cell string electrical performance is minimal and is not considered an electrical hazard.

However, there is a risk of mechanical fouling in the retraction or re-deployment of aged solar array blanket assemblies and the solar array mast. If the array gets stuck in a partially retracted or deployed state, the mast may not have sufficient strength capability to handle space shuttle orbiter docking loads. If this is the case, then the stuck array must be jettisoned. The baseline jettison procedure requires an ISS crew of at least 3 people: 2 crew members on EVA and 1 crew member inside the ISS to operate the ISS Remote Manipulator System robotic arm. Until the space shuttle program return-to-flight milestone is achieved, the ISS has only a 2 person crew. Under this circumstance, the solar array jettison procedure is not feasible which makes retracting the solar array for SSU R&R not feasible.

Therefore, the ISS Program Office is refining the procedure for SSU R&R EVA undertaken with SAWs fully deployed. This refined procedure includes disconnecting the SAW power connectors to the SSU input and places SAW solar cell strings in an open-circuited condition. Since the SSU R&R EVA can not be completed during one orbital eclipse period, the crew will insert a shunt plug to collapse solar array string voltage levels during orbital sun periods. Although EVA procedures are performed during eclipse, the cold SAW strings are exposed to several types of non-solar, weak light sources.

Natural weak light sources include moonlight, meteor ionization trails, lightning, sprites, elves and supernovae. Of these light sources, only moonlight was assessed. The latter sources were eliminated from further consideration due to their low probability and short-lived, transient nature.

Artificial weak light sources on the ISS exterior include Video Camera Luminaires (VCLs), Crew/Equipment Translation Aid (CETA) Lamps, and Extravehicular Mobility Unit (EMU – i.e., space suit) helmet lights. Figure 1a shows a schematic diagram and photograph of a VCL light source. Figure 1b shows the location of ISS camera ports (CP) with attendant VCLs. Figure 1c shows on-orbit photographs of a functioning VCL on the S1 truss segment. Figure 2 shows a composite photograph of EMU helmet lights.

Artificial and natural weak light sources can produce enough light to energize solar array strings and present a potential current and/or voltage hazard to EVA crew members and ISS hardware during SSU R&R activities. This report documents test data and analyses to quantify solar array string electrical performance under highly off-nominal, LILT (low-temperature, low-intensity) operating conditions with non-solar light sources.

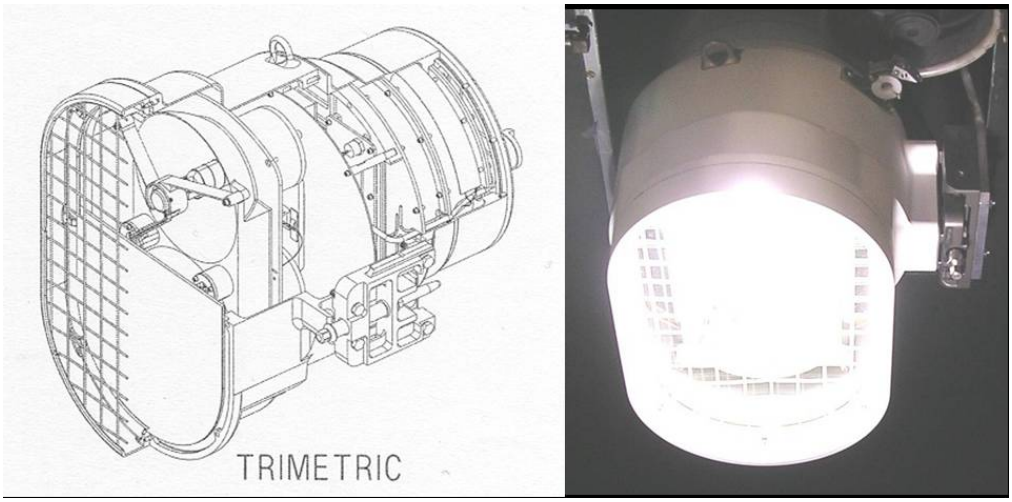

Figure 1a.—ISS Video Camera Luminaire (VCL) schematic drawing (McDonnell Douglas, 1F01194-1) and photograph.

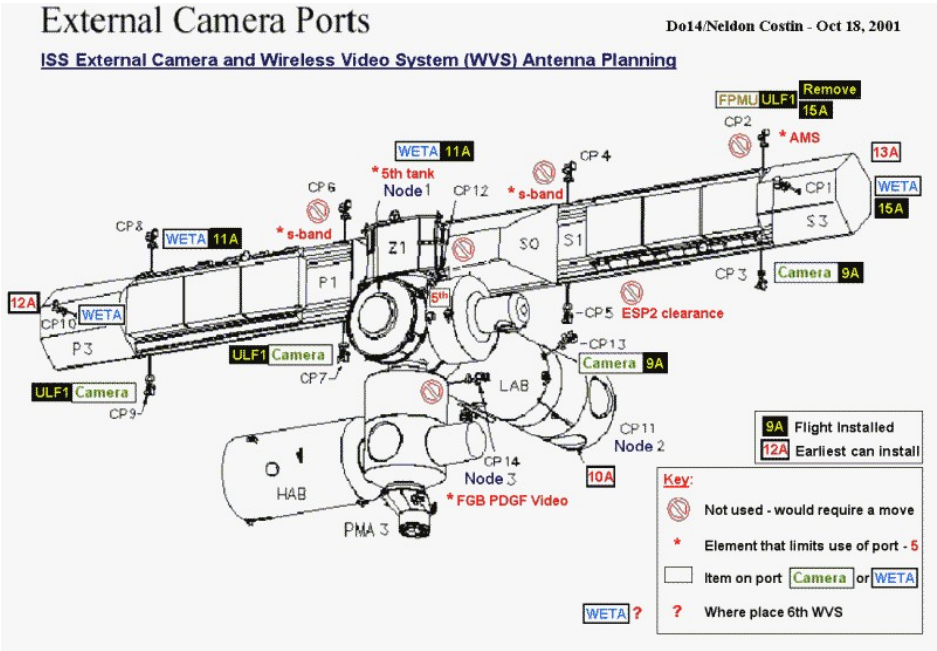

Figure 1b.—ISS camera locations.

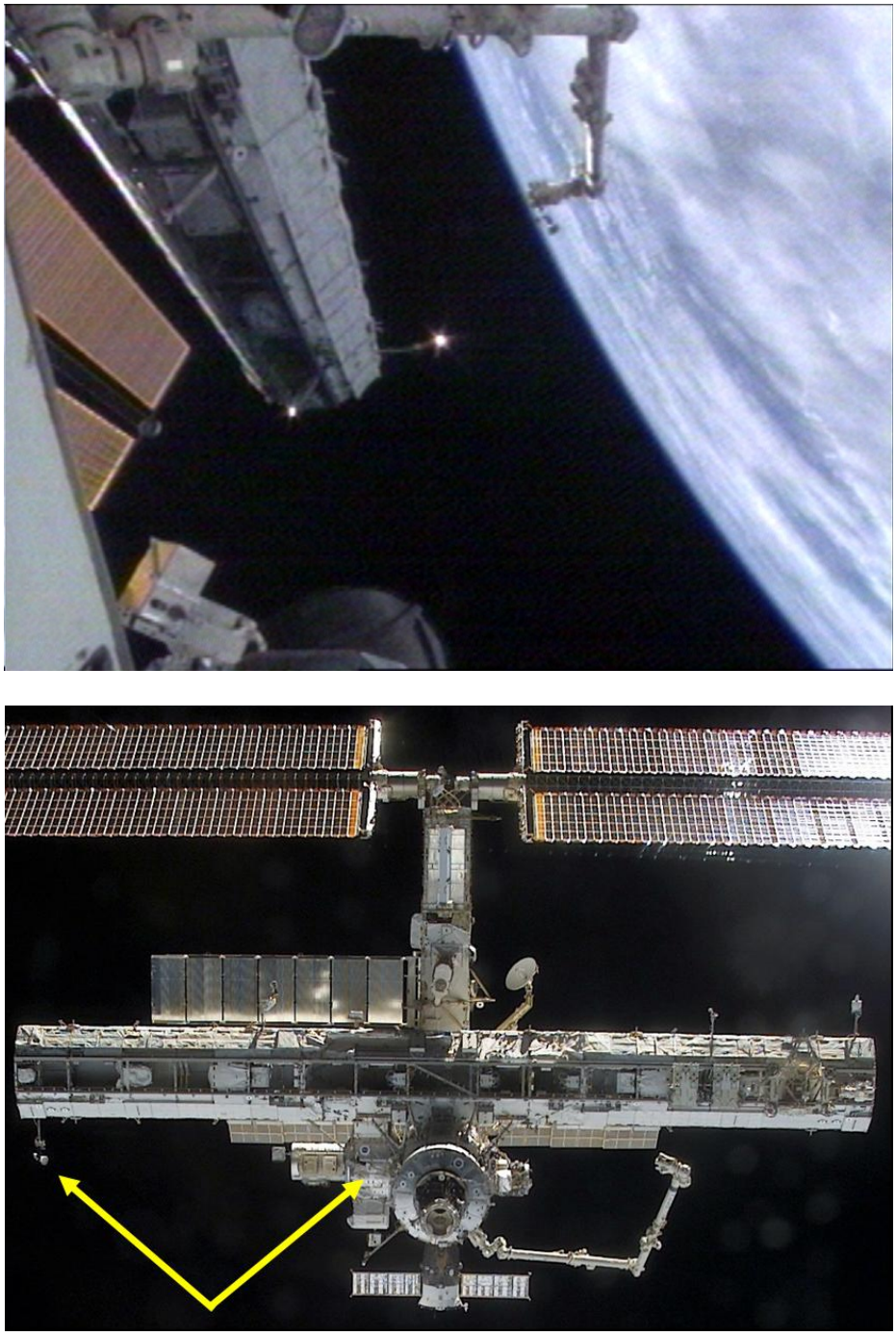

Figure 1c.—ISS on-orbit photographs of S1 and US lab module “Destiny” VCLs.

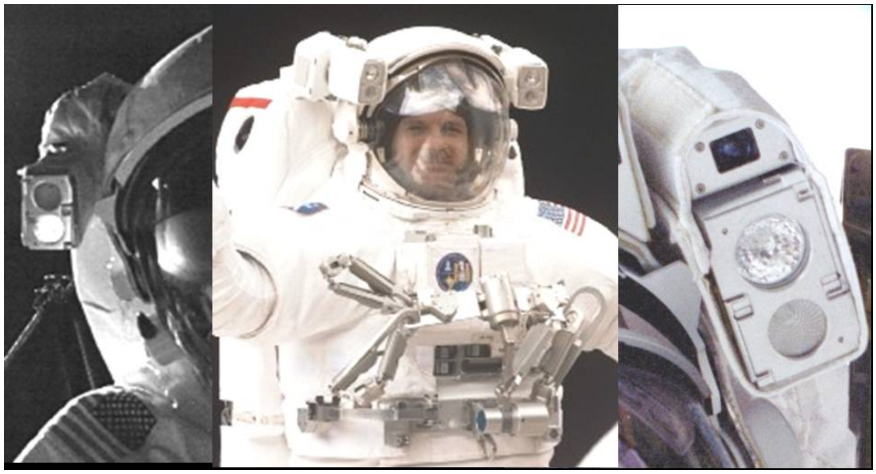

Figure 2.—Composite photograph of EMU helmet lights.

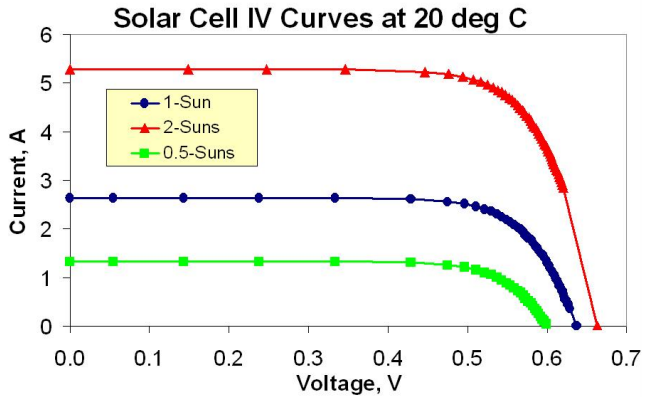

Figure 3a.—Effect of light intensity on solar cell current-voltage response.

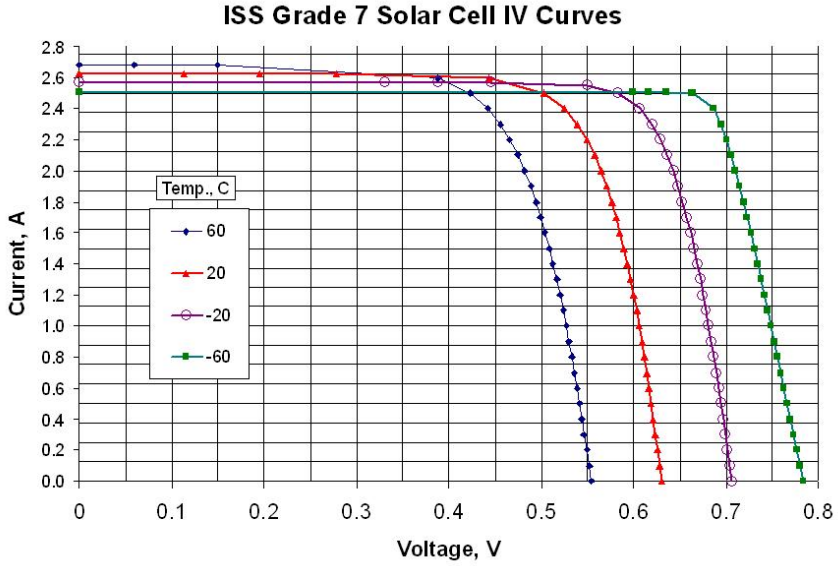

Figure 3b.—Effect of temperature on solar cell current-voltage response.

$$I = I_{SC} - I_0\left[e^{\frac{q(V - IR_s)}{\gamma kT}} - 1\right] - \frac{V}{R_{sh}}$$

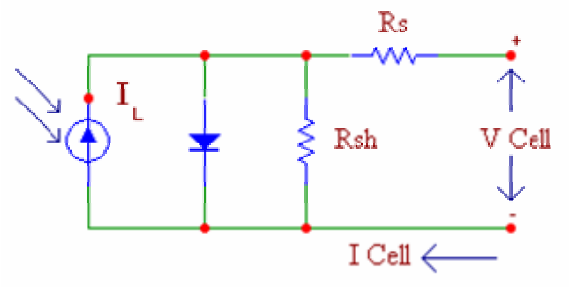

γ = Curve fitting parameter(Ideality factor)
I = Cell Current
k = Boltzmann constant
I_0 = Cell diode saturation current
q = Electron unit charge
R_s = Cell series resistance
R_{sh} = Cell shunt resistance
T = Absolute cell temperature
V = Cell Voltage

Figure 4.—Simplified solar cell electrical model schematic.

1.1 LILT Basics

Solar cells exhibit a reasonable and predictable behavior over a wide range of operating temperatures and light illumination intensities. As shown in Figure 3a, the solar cell short-circuit current (Isc) is generally proportional to light intensity while open-circuit voltage (Voc) is generally proportional to the natural logarithm of Isc. The primary solar cell temperature effect is increased bandgap energy at reduced temperature (Ref. 1). This has the combined effect of increasing cell voltages while decreasing cell current output (Fig. 3b).

As the solar cell operating temperatures and light intensities become very low, potential unexpected performance behaviors can occur (Refs. 2 to 5). For example, with low solar intensity, the photo-generated current, I_L, becomes increasing smaller compared to the nominal shunt current and diode saturation current (see Fig. 4 for a simplified solar cell electrical model schematic) and solar cell current and voltage output capacity drops substantially. At very low temperatures, moderately doped rear contacts (ohmic at nominal operating temperature) can exhibit Schottky behavior and cause a substantial solar cell voltage loss. Also at very low temperatures, metals can come out of solution form metal-like semiconductors and/or dendritic growth under front contact metallization. Both of these result lead to solar cell current and fill factor losses. Through careful design, all of these solar cell performance LILT issues can be effectively addressed. However, ISS solar cells were not specifically designed for LILT tolerance and therefore, must be tested to determine their LILT performance characteristics.

2.0 Approach

The approach to assess SAW string electrical performance during a refined SSU R&R EVA procedure was 4-fold. First, solar cell LILT test data was obtained with several low-intensity light sources. Second, an orbital eclipse lighting analysis was performed to calculate light intensity on SAWs for several scenarios. Third, SAW string electrical performance was calculated based on the calculated values of eclipse lighting intensity and measured values of solar cell performance on LILT conditions. Fourth, and lastly, calculated SAW string current and voltage capabilities were compared to safe values determined for EVA crew and ISS hardware.

Safe current-power levels to avoid a molten metal hazard with connector pins are less than 3-amp per pin and less than 180-watt per pin (Refs. 6 and 7). To avoid SAW electrostatic discharge (ESD) trigger arcs to the space plasma, negative solar cell voltage must not exceed -200-volts (Refs. 8 and 9). To avoid SAW cell-to-cell sustained arcs, solar cell-to-cell differential voltage times the string current capacity must not exceed 40-watts for closely spaced cells (gap size of 1.0×10^{-3} m). Safe current-voltage levels to avoid human shock are less than 32-volt and less than 0.001-amp (Refs. 6, 7, and 10).

3.0 Test Plan

3.1 Test Articles

Six available ISS silicon solar cells (Spectrolab k6700B) (Ref. 11) were used in LILT testing (Fig. 5). Each cell was marked with a serial number and a grade level for traceability. Three of these were "grade 5" cells (serial numbers 2532, 2570, 2574) and three were "grade 8" cells (serial numbers 3055, 3060, 3193). After manufacture, solar cells are graded 1 to 11 by the current level produced at a 0.495-volt operating voltage. The SAW specification calls for the SAW circuits to have an average grade level of 7 or above. These individual cells were obtained from spare Photovoltaic Panel Modules (PPMs) from the US-Russian Mir Cooperative Solar Array (MCSA) program (Refs. 12 and 13).

ISS solar array technology panels, with 80 series-connected solar cells mounted to a flexible Kapton-scrim composite panel material, were also used in LILT testing. For example, panel #1083, manufactured by Lockheed-Martin, is a "grade 7" spare PPM unit from the MCSA program. Figure 6 shows an electrical schematic and photographs of the PPM #1083 test article.

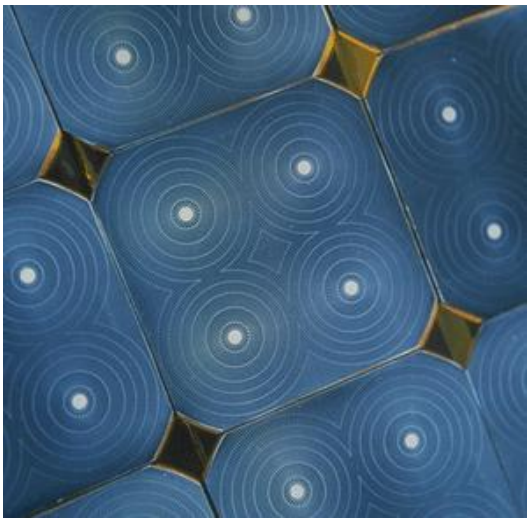

Figure 5.—8 by 8-cm Spectrolab k6700B (ISS) silicon solar cells.

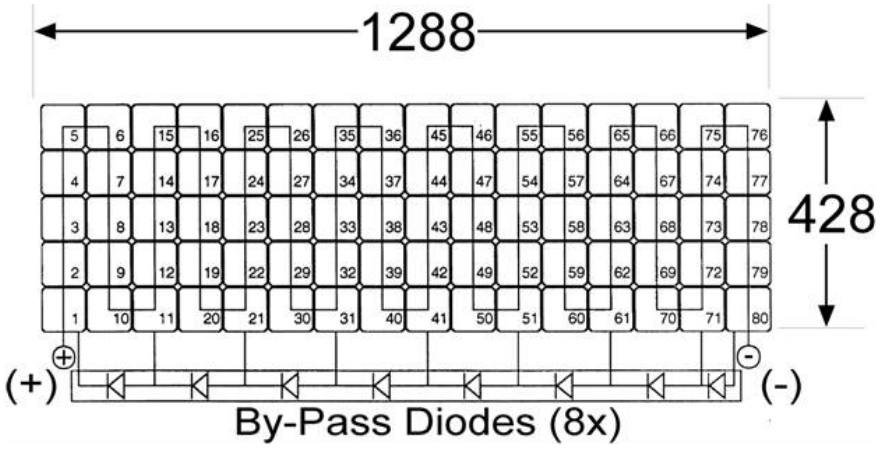

(a) Physical and electrical schematic (dimensions in mm).

(b) Photograph—front side (solar cells).

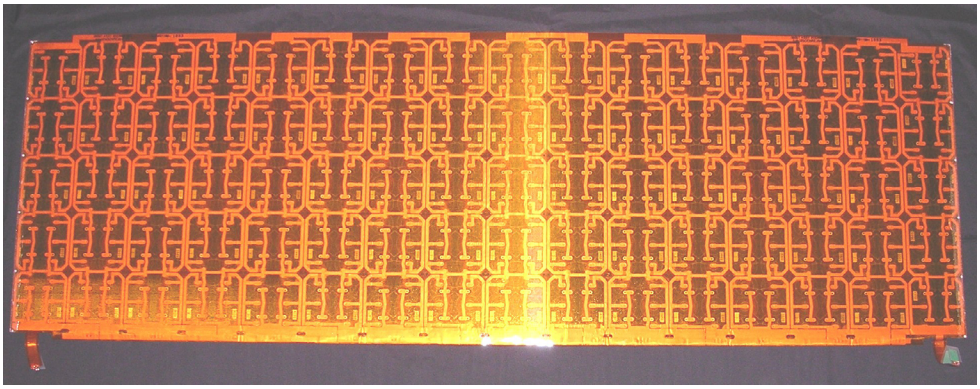

(c) Photograph—backside (Kapton-scrim panel).

Figure 6.—MCSA spare PPM #1083.

3.2 Light Sources

Panel ambient current-voltage measurements were obtained with illumination from the full (or nearly full) moon on April 5–6, 2004 and on May 5–6, 2004. Specific test information is provided below in Table 1.

The intensity of full moon illumination is on the order of millionth's of Suns (1 Sun = 1371 W/m^2). The spectrum of moon light in Earth orbit is obtained by convolving the AM0 solar spectrum with the lunar spectral reflectance shown in Figure 7. The spectrum of moon light on the Earth's surface must be further convolved with atmospheric transmittance as a function of effective air mass. The integrated loss in light intensity has been estimated and is shown in Table 1.

Table 1.—Full Moon Test Conditions

Test Date	April 5–6, 2004	May 5–6, 2004
Sky Condition	Clear	Clear
Test Location	Strongsville, OH	Cleveland, OH
Ambient Temperature	–4 °C	+10 °C
Local Lunar Transit Time (Test performed <2-hr from Lunar Transit)	2:12 AM (4/6/2004)	2:44 AM (5/6/2004)
Lunar Zenith Angle (0° is overhead)	42°	65°
Effective Atmospheric Air Mass	AM1.34	AM2.40
Integrated Intensity Loss Relative to AM0 Intensity	34 percent	61 percent
Test Articles	15-cell section, grade 7, PPM #1040	80-cell, grade 7, PPM #1083 80-cell, grade 5, PPM #1010
Measurement Instrumentation	Craftsman 82025 high Precision Multimeter	Keithly 2420 Sourcemeter, NEC Versa S/50 Laptop PC

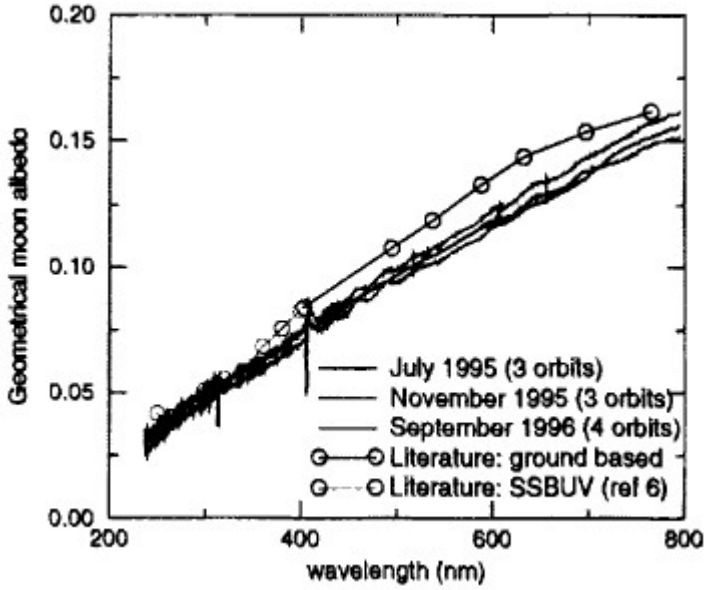

Figure 7.—Spectral reflectance of the Moon. Averaged geometrical Moon albedos measured by GOME from July 1995, November 1995, and September 1996 (Ref. 14).

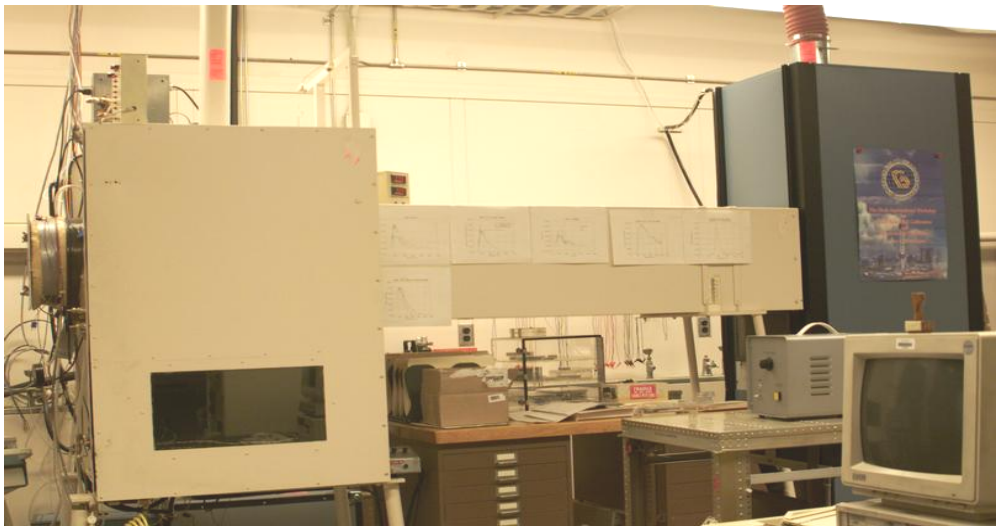

Figure 8a.—X-25 solar simulator at NASA Glenn (light source on the right; test chamber on the left).

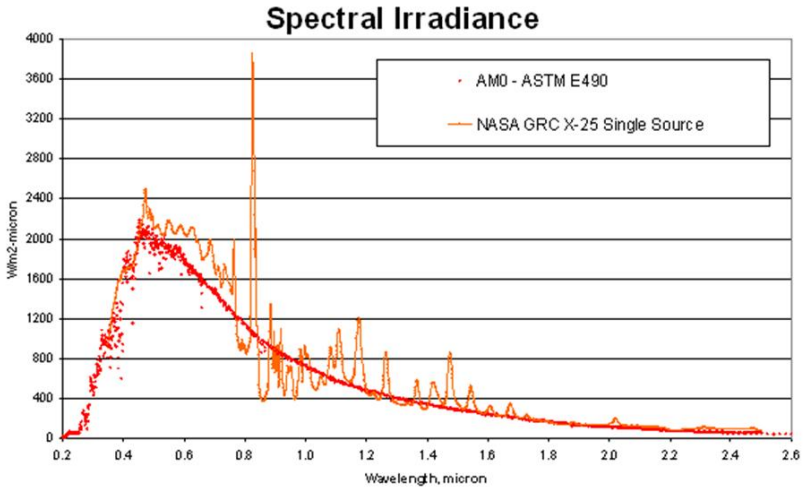

Figure 8b.—X-25 solar simulator spectrum.

Individual cells were tested using the industry standard, Spectrolab X-25 Mark II, constant light solar simulator (Refs. 15 and 16) shown in Figure 8a. Using a xenon arc lamp, the X-25 closely replicates the AM0 solar spectrum and intensity (see Figure 8b). Based on past measurements, the uniformity of X-25 light intensity across the solar cell test plate was within ±0.5 percent.

Individual solar cell LILT tests and 80-cell panel ambient tests were conducted using the VCL light source produced by McDonnell Douglas Corp. (Drawing #1F01194-1). The VCL, shown in Figure 1a, is 0.44-m deep, 0.41-m (maximum) across the dual-lamp ellipsoidal face and has a mass less than 15.5-kg (Ref. 17). It operates at an input voltage of 120-volts DC and nominally draws about 190-watts of power. The VCL can be operated in a hard vacuum or in an ambient laboratory environment and can be positioned ~1-m away from the solar cell under test to provide about 1/4th-Sun intensity. Figure 9a shows the measured VCL illumination uniformity

on 23 by 23 square-foot grid located 18.3-m from the VCL. These data indicate there is a large variation, +41/–57 percent, about the mean 5.2-footcandle illumination intensity value. A foot-candle of light at 555-nm wavelength is equal to approximately 0.0157 W/m^2. After successfully processing an Avionics Equipment Request to the ISS Avionics Equipment Panel, the qualification VCL unit located at NASA Kennedy Space Center was shipped to NASA GRC to support this testing program. Figure 9b shows a photograph of the VCL during solar cell LILT testing.

VCL VideoPhotometric Data at 18.3-m (foot-candles on 23x23 square foot grid)

3.13	3.56	3.84	4.04	4.23	4.35	4.39	4.43	4.58	4.66	4.55	3.96	3.62	3.40	3.36	3.29	3.20	3.10	2.93	2.76	2.58	2.41	2.27
3.60	4.02	4.29	4.49	4.53	4.65	4.60	4.69	4.80	4.91	4.58	4.41	3.78	3.64	3.64	3.58	3.49	3.36	3.18	3.01	2.86	2.72	2.54
4.04	4.52	4.63	4.72	4.83	4.89	4.92	4.97	4.98	5.15	4.84	4.47	4.31	4.19	4.00	3.84	3.82	3.60	3.49	3.31	3.14	3.01	2.85
4.32	4.69	4.83	4.87	4.96	5.04	5.06	5.09	5.10	5.20	5.06	4.78	4.81	4.79	4.46	4.29	4.24	3.95	3.81	3.68	3.51	3.34	3.16
4.56	4.80	4.99	5.10	5.07	5.02	5.06	5.13	5.27	5.38	5.35	5.09	4.93	4.85	4.79	4.81	4.59	4.36	4.16	3.98	3.85	3.74	3.56
4.58	4.95	5.09	5.19	5.04	4.98	5.07	5.22	5.34	5.45	5.48	5.31	5.07	5.06	5.11	5.09	4.94	4.70	4.50	4.28	4.09	4.14	4.00
4.54	4.96	5.13	5.17	5.00	5.00	5.13	5.19	5.28	5.39	5.46	5.32	5.15	5.20	5.24	5.27	5.22	5.04	4.81	4.60	4.39	4.48	4.31
4.74	4.97	5.14	5.08	5.02	5.09	5.18	5.22	5.28	5.31	5.35	5.26	5.13	5.21	5.32	5.41	5.41	5.33	5.22	4.93	4.71	4.67	4.52
4.87	5.10	5.16	5.06	5.02	5.09	5.17	5.26	5.25	5.31	5.43	5.38	5.21	5.28	5.41	5.54	5.66	5.69	5.58	5.30	4.95	4.84	4.69
5.06	5.23	5.14	5.06	5.05	5.04	5.15	5.28	5.43	5.58	5.68	5.58	5.46	5.42	5.58	5.74	5.87	5.98	5.89	5.60	5.20	5.02	4.95
5.21	5.37	5.25	5.10	5.05	5.04	5.20	5.39	5.72	6.05	6.18	6.14	5.98	5.82	5.85	5.94	6.03	6.12	6.06	5.85	5.38	5.18	5.14
5.92	5.94	5.80	5.62	5.56	5.48	5.60	5.83	6.29	6.73	6.92	6.80	6.60	6.21	6.06	6.02	6.11	6.14	6.13	5.92	5.47	5.19	5.24
6.25	6.34	6.26	5.99	5.79	5.76	5.90	6.09	6.51	7.02	7.24	7.36	6.91	6.30	5.95	5.92	5.96	5.92	5.82	5.68	5.36	5.09	5.13
6.10	6.36	6.39	6.04	5.78	5.78	5.85	6.02	6.36	6.81	6.98	7.20	6.86	6.32	6.00	5.90	5.94	5.85	5.76	5.57	5.45	5.20	5.20
5.81	6.10	6.34	6.14	5.86	5.77	5.76	5.89	6.10	6.31	6.45	6.79	6.64	6.25	6.00	5.87	5.86	5.73	5.61	5.41	5.19	5.25	5.13
5.57	5.90	6.29	6.29	5.98	5.82	5.74	5.85	5.97	6.01	6.03	6.36	6.40	6.21	6.07	5.96	5.86	5.66	5.48	5.26	5.16	5.15	4.97
5.49	5.81	6.15	6.36	6.18	5.93	5.78	5.84	5.90	5.88	5.86	6.26	6.38	6.21	6.08	5.98	5.86	5.65	5.46	5.37	5.27	5.08	4.84
5.23	5.59	5.92	6.28	6.22	6.14	5.92	5.83	5.87	5.85	5.80	6.19	6.41	6.30	6.10	5.93	5.83	5.66	5.56	5.39	5.24	5.06	4.71
4.89	5.33	5.74	5.99	6.12	6.28	6.23	6.12	6.02	5.91	5.82	6.19	6.37	6.27	6.10	5.97	5.90	5.83	5.59	5.48	5.27	4.99	4.54
4.23	4.80	5.33	5.70	5.88	6.17	6.35	6.24	6.22	6.11	6.04	6.28	6.45	6.33	6.13	6.05	5.95	5.78	5.63	5.42	5.21	4.84	4.28
3.36	3.84	4.48	5.14	5.47	5.87	6.04	6.16	6.12	6.13	6.12	6.37	6.43	6.39	6.28	6.01	5.90	5.66	5.52	5.28	4.99	4.58	3.96
2.85	3.08	3.52	4.10	4.64	5.15	5.57	5.70	5.76	5.83	5.98	6.18	6.34	6.25	6.02	5.85	5.65	5.48	5.28	4.99	4.65	4.13	3.50
2.58	2.66	2.96	3.40	3.81	4.23	4.63	4.91	5.17	5.41	5.50	5.80	5.90	5.78	5.69	5.55	5.33	5.13	4.90	4.55	4.12	3.57	2.98

Figure 9a.—Measured VCL illumination uniformity at 18.3-m distance (foot-candles).

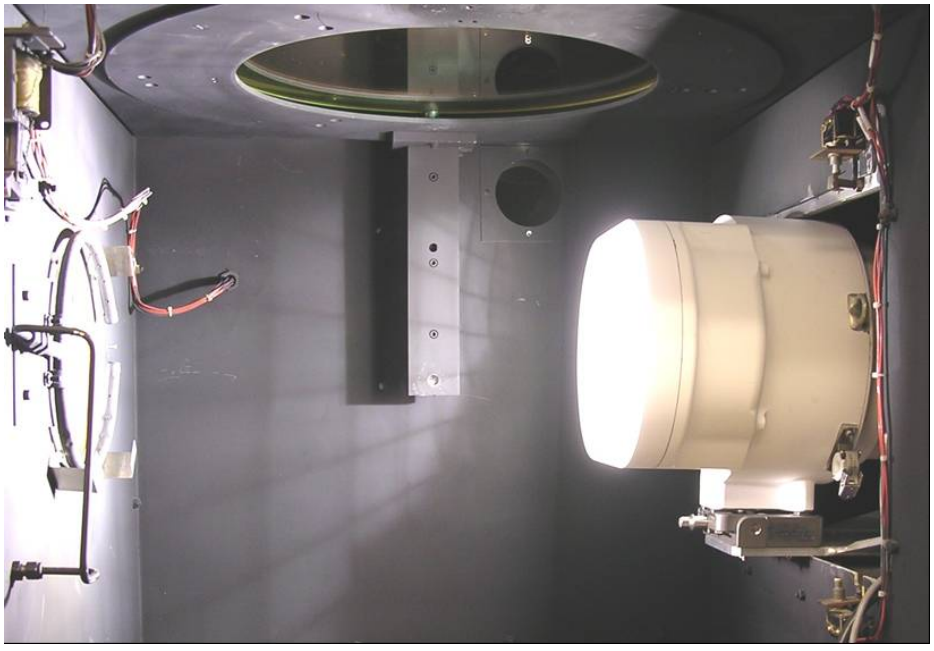

Figure 9b.—Operating VCL during LILT testing.

3.3 Solar Cell LILT Test Conditions

Solar cell LILT testing was performed with effective insolation intensities from 1.0-Sun (1,371 W/m^2) to 0.0001-Sun and solar cell operating temperatures from +30 °C (ambient) to −110 °C.

3.4 Solar Cell Temperature Control

For LILT testing, solar cells were "vacuum-chuck" mounted to a liquid nitrogen (LN_2) cooled test plate. Test plate, and hence solar cell, operating temperature was controlled by a liquid nitrogen line heater regulated by a bang-bang controller with type-T thermocouple temperature signal feedback. Bleed-off nitrogen was used to purge the test chamber and prevent ice buildup on the solar cells. Bleed-off nitrogen was also directed over the test chamber quartz window to prevent frost formation. Figure 10a shows the solar cell LILT testing schematic configuration (Ref. 2) and Figure 10b shows an ISS solar cell mounted on the test plate.

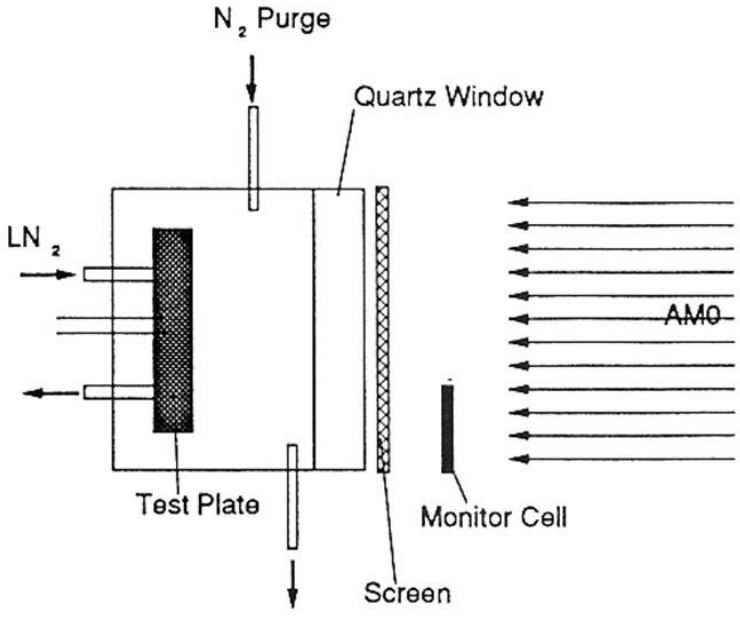

Figure 10a.—Solar cell LILT test configuration (Ref. 2).

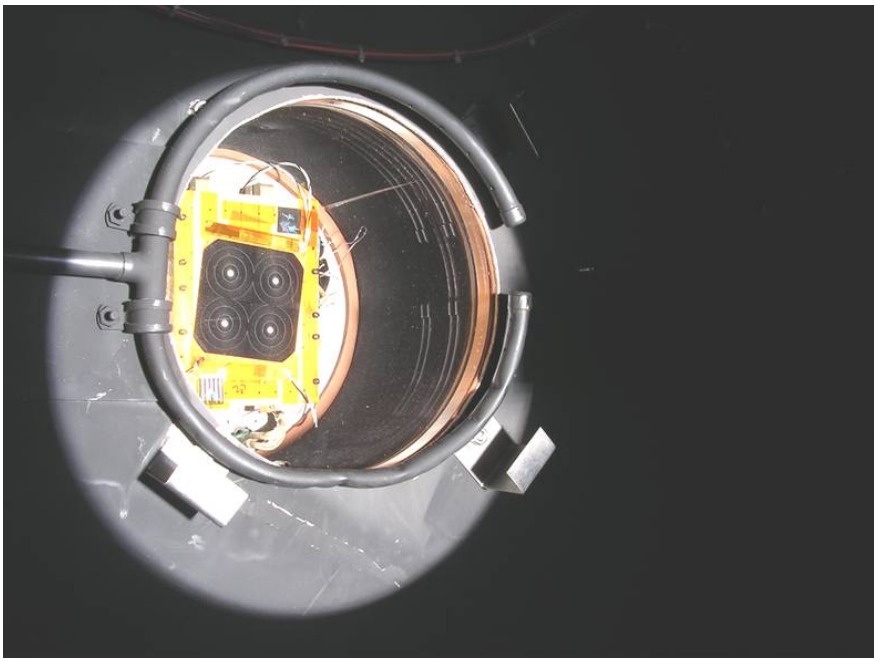

Figure 10b.—Solar cell mounted to LILT test cold plate.

Figure 11.—Solar cell LILT test intensity reducing screen.

3.5 Solar Cell LILT Testing Illumination Intensity Control

The intensity of illumination on the solar cell test plate was controlled by placing one or more screens in front of the test chamber quartz window (Fig. 10a). The screening, shown in Figure 11, acts as a neutral density filter and does not affect the light spectrum on the solar cells.

The intensity reduction of various screens and combination of screens was measured using two methods. The first method made use of calibration standard solar cell short-circuit current (Isc) output with and with out the screening in front of the light source. Over a wide range of intensities, the solar cell Isc is directly proportional to the incidence light intensity. The screening light transmission fraction was determined by dividing Isc-with-screen measurement by the Isc-without-screen measurement. The second method used a radiometer to measure the total light source heat input before and after screen placement. The screening light transmission fraction was determined by dividing the heat-with-screen measurement by the heat-without-screen measurement. Table 2 summarizes the achievable intensity reductions (shown as effective Suns) by various screens or screen combinations and the resulting Isc expected from an ISS solar cell.

Table 2.—LILT Test Screening Intensity Reductions

	X-25		VCL	
Screen	Intensity (Suns)	Est. Cell Isc, A	Intensity (Suns)	Est. Cell Isc, A
None	1.00000	2.6950	0.22000	0.5950
A	0.01700	0.0458	0.00374	0.0101
B	0.02800	0.0755	0.00616	0.0167
C	0.08000	0.2156	0.01760	0.0476
A&B	0.00047	0.0013	0.00010	0.0003

3.6 Test Equipment

Solar cell voltage biasing for LILT testing was provided by an HP6129C digital voltage source. An Eppley Absolute Cavity Radiometer with 0.5-cm^2 aperture was used to measure LILT testing light source intensity with and without light blocking screens. The radiometer thermal power measurement uncertainty was ±1.5 percent.

For ambient panel testing, a Keithley 2420 Sourcemeter was used to bias the solar cell string and sweep the operating current-voltage curve. Control and data collection functions were performed by an NEC Versa S/50 Laptop PC operating Qbasic software.

The VCL was powered by a Sorensen DCS150-7E VCL power supply. VCL relative spectral radiance was measured using an Analytical Spectral Devices Inc., FieldSpec Spectroradiometer. Solar cell spectral response was measured with the Oriel Model 66070 Xenon Arc Solar Simulator (Fig. 12) with 46, 2-inch filters and a spectral range of 350 to 1900-nm at 10-nm intervals. The instrument has a ±3 percent absolute measurement uncertainty and provides an integrated solar cell Isc value within 5 percent of that directly measured.

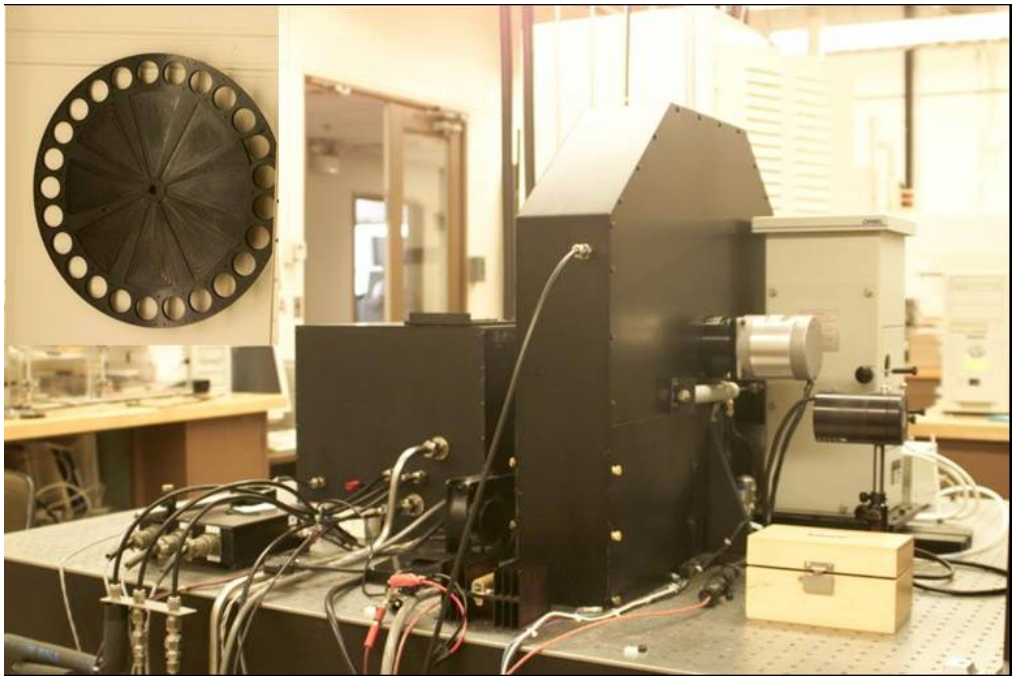

Figure 12.—Solar cell spectral response instrument (Oriel 66070).

3.7 Test Instrumentation

During LILT testing, a monitor solar cell and standard reference solar cell were used to verify the integrity of illumination of the solar cell test plate. The simulator 1-Sun intensity was set using a calibrated standard solar cell of like material (performance characteristics). The silicon standard reference cell "A-161" has been flown on an aircraft or balloon to high altitude where its electrical performance has been measured periodically over the last 20-years. These high-altitude data can then be reliably extrapolated to obtain AM0 illuminated performance (Ref. 18).

With the standard reference cell calibrated light intensity, a monitor cell was used to maintain the nominal light intensity and adjust for temporal stability in the arc lamp (flicker). At each current-voltage point, the test cell current, test cell voltage and monitor cell current were all measured simultaneously (after a trigger signal). The test cell current was then corrected by the ratio of the monitor cell current/calibrated monitor cell current. The measurements are recorded at a ~40 Hz sampling rate with an average of 16 measurements per point. Based on the monitor solar cell and calibrated, standard reference cell, the LILT test X-25 light source intensity magnitude and uniformity was controlled with an uncertainty of less than ±0.5 percent.

LILT test solar cell and cold plate temperatures were measured by type-T thermocouples with an uncertainty of ±1 °C. Solar cell temperature was typically maintained within 2 °C during a current-voltage data test point (Ref. 2). The test cell temperature was determined by a thermocouple attached to the front side of a "witness" cell (non operational cell of similar characteristics). The witness cell temperature was measured at the beginning and end of each current-voltage (I-V) curve. Solar cell I-V data were measured using Kelvin probes and 4-wire connection to Fluke 8505 and Fluke 8520 digital multimeters. The uncertainty in measured solar

cell current was ±0.1 percent while that of solar cell voltage was ±0.01 percent. Ambient panel test current and voltage measurement were made using a 4-wire technique with a ±0.015 percent uncertainty.

3.8 Test Procedures

A. LILT Tests

A summary of LILT test procedures using the X-25 or VCL light sources are provided below:

(1) Mount ISS solar cell and calibration cells to cold plate; install sensors/probes
(2) Establish 1-sun illumination light source and cell room temperature thermal equilibrium
(3) Measure and record cell I-V curve and temperature
(4) Mount flux reduction screen(s), measure/record cell I-V curve and temperature after stabilizing
(5) Repeat step (4) for all screens
(6) Adjust LN_2 heater power to establish next lower test temperature. Repeat steps (2) to (5).
(7) Repeat steps (2) to (6) for all decreasing test temperatures points
(8) Repeat steps (2) to (7) for all increasing test temperatures points back to room temperature
(9) Mount next test solar cell and repeat steps (2) to (8).
(10) Repeat steps (1) to (9) for all test solar cells

B. Panel Full Moon Test

A summary of solar cell panel (80-cells) ambient full moon illumination test procedures are provided below:

(1) Select grade 7 panel PPM #1083 to test; place out-of-doors to stabilize temperature with the ambient temperature for a 1-hour period
(2) Set up test support equipment: Keithley 2420 Sourcemeter to sweep the I-V curve and NEC Versa S/50 Laptop PC to control and collect data
(3) Connect 4-wire current-voltage probes to panel electrical leads
(4) With moon within ~2-hours of lunar transit (highest elevation angle), manually point panel front side normal to the moon vector; monitor panel Isc and when maximized, hold panel in place. Panel backside is directed toward the ground to minimize backside illumination
(5) Measure panel I-V curve data (includes data and time stamp) and verify data file on PC
(6) Measure panel I-V curve data again and check for consistency
(7) Manually shadow panel from direct moon light and measure panel I-V curve data set (used to correct data for spurious ambient lighting)
(8) Record ambient temperature (assumed panel temperature)

See Table 1 for more full moon panel testing conditions and information.

C. Panel VCL Test

A summary of solar cell panel (80-cells) ambient VCL illumination test procedures are provided below:

(1) Select grade 7 panel (PPM #1083) used in full moon testing
(2) Position VCL at the end of the laboratory building hallway at midpoint of hallway height and width
(3) Connect Sorensen DCS150-7E power supply
(4) Activate VCL (120-volt DC, 1.57-amps); operate for >30-minutes prior to collecting first panel I-V data set to allow light source to stabilize
(5) Minimize non-VCL lighting in laboratory hallway (turn off lights, block light sources)
(6) Using tape measure, mark off distance increments from VCL position (~3 to ~18-m in ~1.5-m increments; ~±0.025-m accuracy)
(7) Set up test support equipment: Keithley 2420 Sourcemeter to sweep the I-V curve and NEC Versa S/50 Laptop PC to control and collect data
(8) Manually position panel at nearest distance increment from VCL and on the VCL light source centerline (horizontally and vertically). Panel backside is directed away from light source to minimize backside illumination
(9) Position test support equipment by panel
(10) Position black draping on floor centered midway between VCL and panel (minimize floor reflected light)
(11) Connect 4-wire current-voltage probes to panel electrical leads
(12) Measured panel I-V curve data and verify data file on PC
(13) Measure panel I-V curve data again and check for consistency
(14) Manually shadow panel from direct VCL lighting and measure panel I-V curve data set twice (used to correct data for VCL reflected light and spurious ambient lighting); confirm data consistency
(15) Reposition panel and test support equipment to next furthest distance increment; reposition floor black draping
(16) Repeat steps (11) to (15) for all distance increments
(17) Estimate ambient temperature at 27 °C (assumed panel temperature)—ambient temperature was not directly measured.

4.0 Test Results

4.1 Full Moon/Ambient Panel

The current-voltage curve of the 80-cell panel was measured while illuminated with terrestrial full moon light (Fig. 13). These uncorrected data indicate a solar cell Isc of about 4 microamps and a Voc per cell of 1/80th volt.

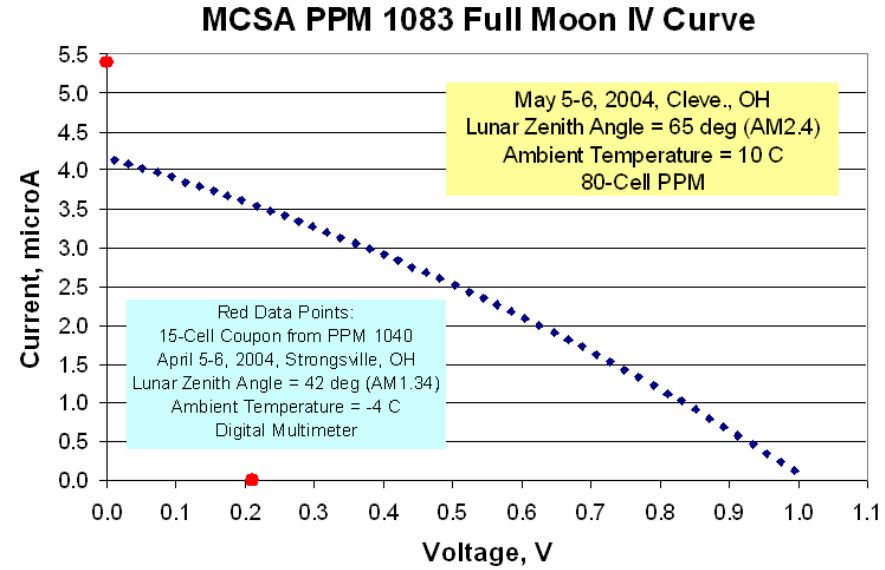

Figure 13.—Panel current-voltage capacity with full moon illumination.

4.2 X-25/Solar Cell LILT

For reference, Figure 14a shows the current-voltage response of grade 5 (#2574) and grade 8 (#3055) ISS silicon solar cells at room temperature (25 °C) under 1-Sun, air mass 0 (AM0) illumination closely approximated by the X-25 solar simulator.

Figure 14b to f shows a series measured current-voltage curves for a grade 8 solar cell (#3060) with either temperature or effective X-25 illumination intensity as a parameter. Plots have either a linear current axis or a logarithmic current axis (for clarity).

It is clear from Figures 14d and 14f that at the low effective intensity of 0.00047-suns, the solar cell has lost its photodiode characteristic: that is, it exhibits an extended flat current leg and it lacks a meaningful Voc value (greater than 0.5-volts).

Since Isc and Voc are the solar cell data of most interest, these values are displayed in the following plots. Figure 15a shows the response of a grade 5 solar cell (#2532) Isc versus temperature from approximately –100 to 20 °C and with illumination intensity as a parameter. The illumination level varied from 1-Sun to 0.0005-Suns. Further reductions in flux level, while maintaining good illumination uniformity, was not attainable using the screens. At 0.0005-Suns, the flux level is about 2.5 times higher than the best-case (VCL, ISS-15A case) eclipse light level calculated. Typical coldest sun-tracking solar array temperatures are in the range of –80 °C and occur near the eclipse exit of a zero solar beta angle orbit (orbit with the maximum eclipse period).

The solar cell Isc response is generally well behaved: that is, the magnitude of Isc is proportional to the illumination intensity and Isc increases monotonically with increasing temperature. The only exception to this is for the lowest flux intensity of 0.0005 Suns, where Isc actually decreased ~33 percent over the temperature range from –100 to 20 °C (Fig. 15b).

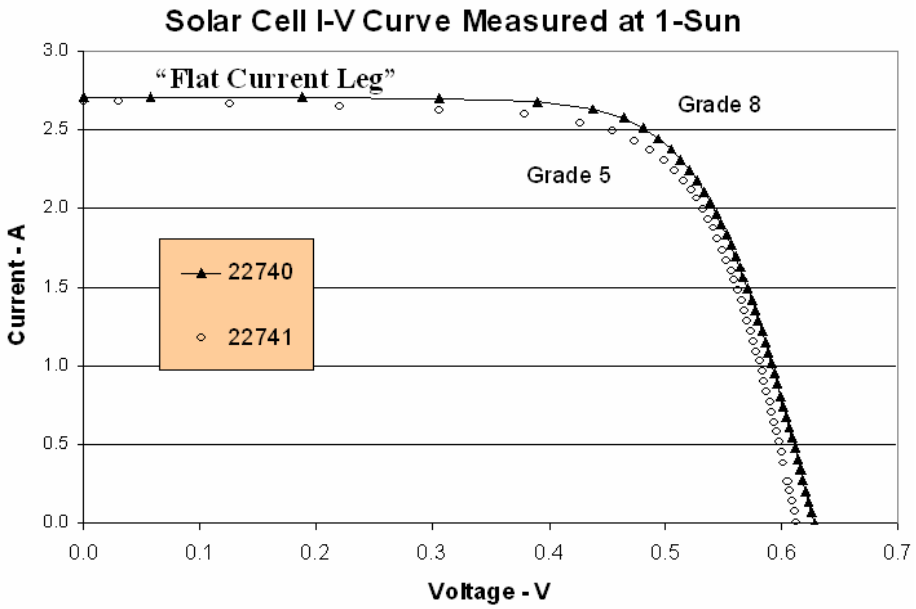

Figure 14a.—ISS solar cell current-voltage curve—1-Sun X-25 illumination (25 °C).

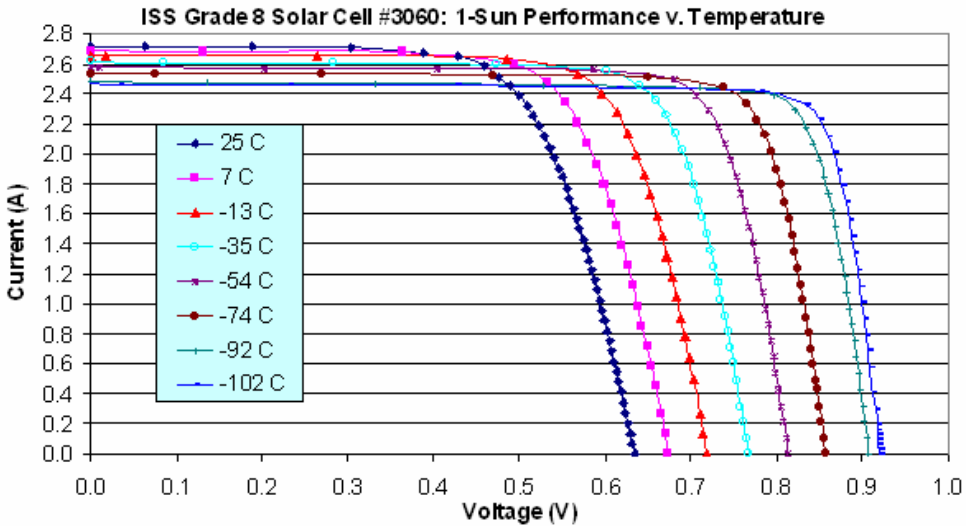

Figure 14b.—ISS solar cell current-voltage curve 1-Sun X-25 illumination (various temperatures in °C).

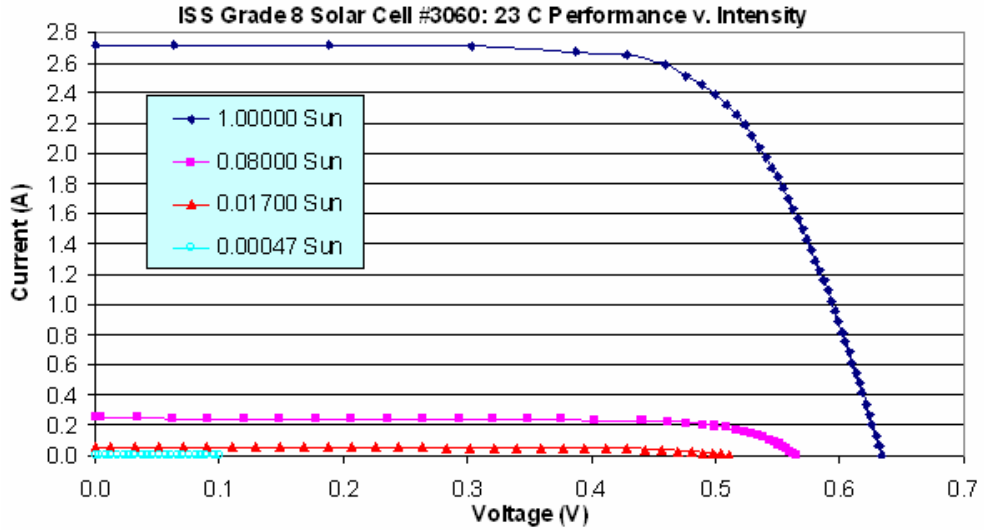

Figure 14c.—ISS solar cell current-voltage curve room temperature (various illumination intensities).

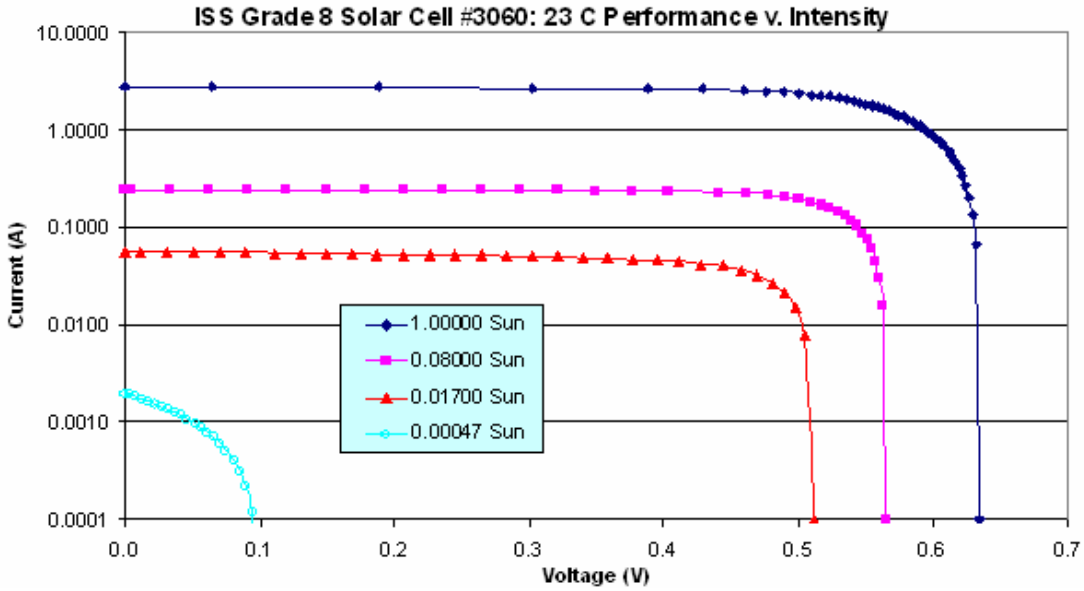

Figure 14d.—ISS solar cell current-voltage curve (log axis) room temperature (various illumination intensities).

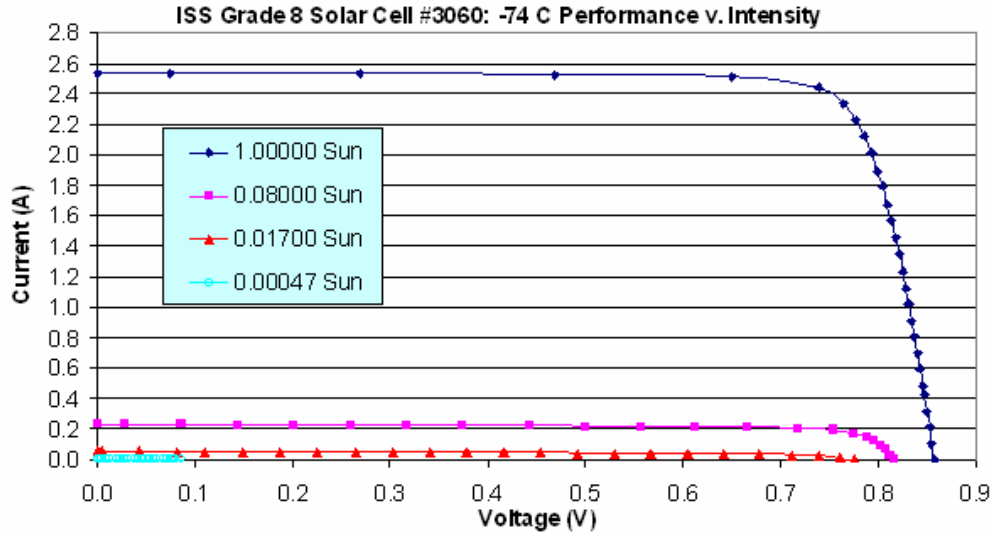

Figure 14e.—ISS solar cell current-voltage curve –74 °C temperature (various illumination intensities).

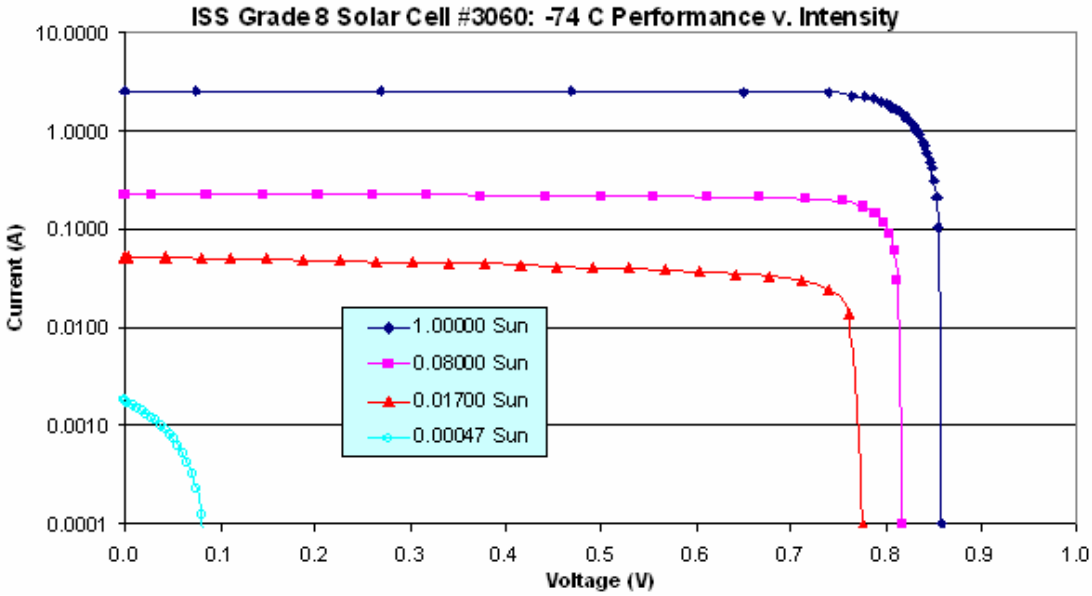

Figure 14f.—ISS solar cell current-voltage curve (log axis) –74 °C temperature (various illumination intensities).

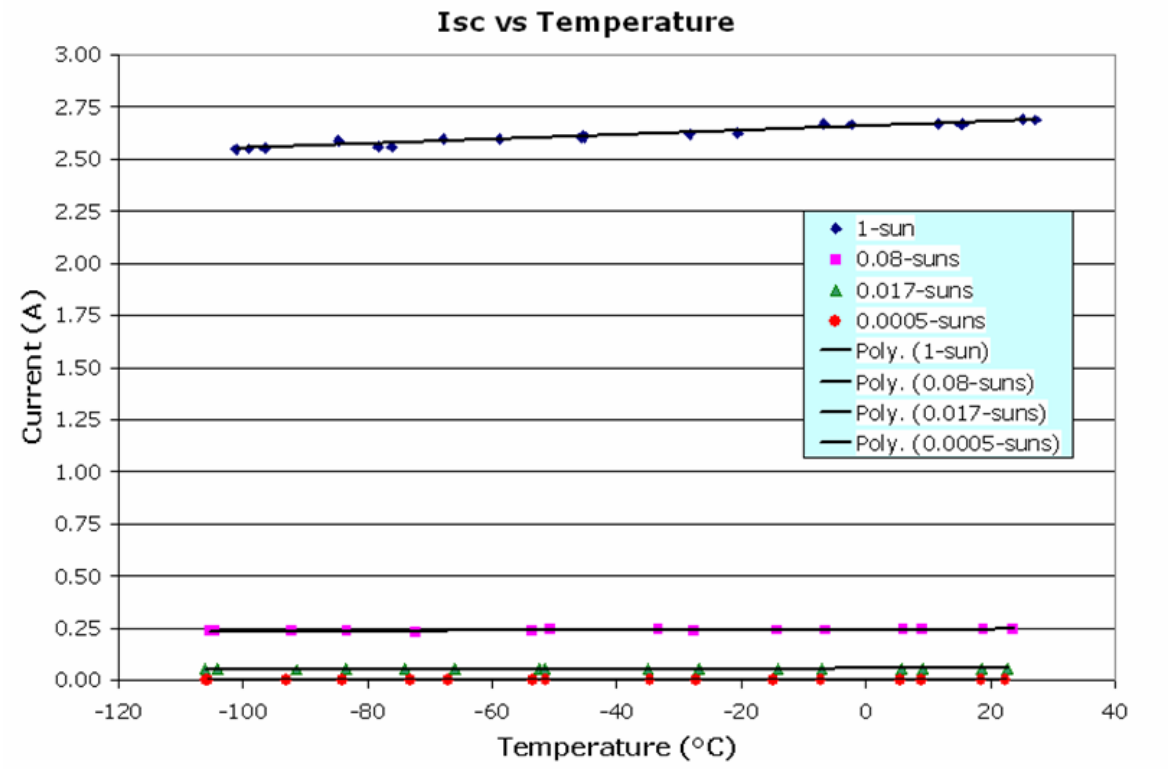

Figure 15a.—ISS solar cell Isc – X-25 LILT conditions.

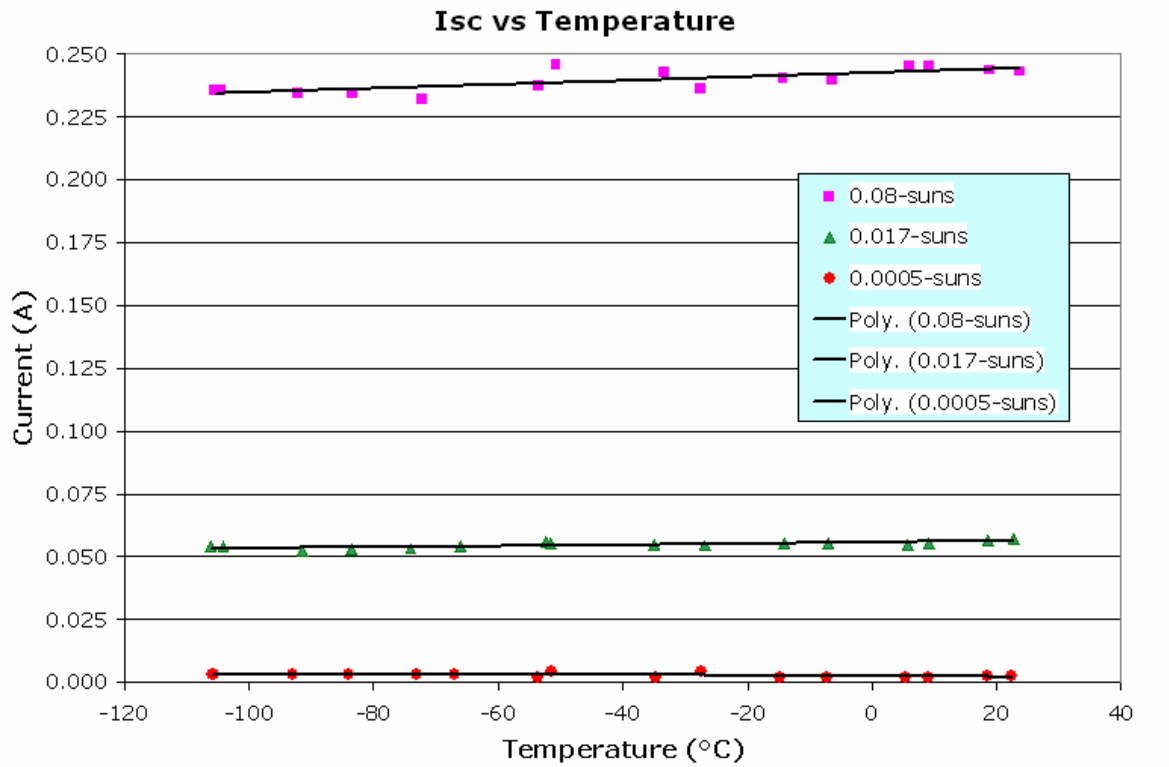

Figure 15b.—ISS solar cell Isc – X-25 LILT conditions (reduced current scale).

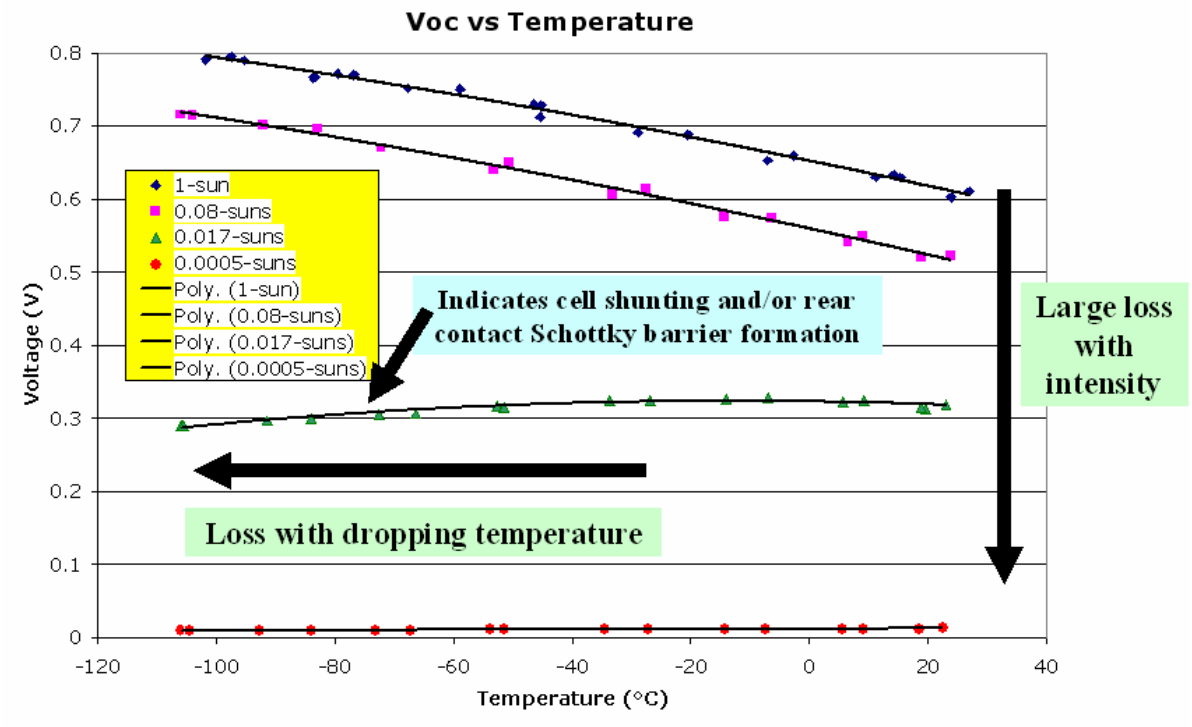

Figure 16.—ISS solar cell Voc – X-25 LILT conditions.

Figure 16 shows how a grade 5 solar cell (#2532) Voc varies with temperature and with illumination intensity as a parameter. At 1-Sun and 0.08-Suns intensity, the Voc response is well behaved: that is, the magnitude of Voc varies with the natural logarithm of intensity and Voc decreases monotonically with increasing temperature level. At lower intensities of 0.017-Suns and 0.0005-Suns, classic Voc behavior is not observed. Instead, the Voc magnitude drops faster than logarithmic with intensity and Voc actually increases 10 to 25 percent with increasing temperature over the range from –100 to 20 °C.

The reasons for this kind of Voc behavior under LILT typically are relatively high shunt currents and rear contact Schottky barrier formation. At low solar intensity, the photo-generated current, I_L, becomes increasingly smaller compared to the nominal shunt current and diode saturation current (see Figure 4 for a simplified solar cell electrical model schematic). Due to these leakage currents back across the solar cell junction, the cell can not support as high a voltage and Voc drops accordingly. At very low temperatures, moderately doped rear contacts (ohmic at nominal operating temperature) can exhibit Schottky barrier formation and cause a substantial solar cell voltage loss.

These single solar cell test data indicate a counterintuitive conclusion: that is, under low illumination level, Isc is highest at low temperature while Voc is highest at high temperature.

4.3 VCL/Solar Cell LILT

Solar cell LILT testing was continued using a Video Camera Luminaire (VCL) as the light source. The VCL source strength is about 5 times lower than that of the X-25 solar simulator. Thus, illumination intensities varies from 0.22-Suns to 0.0001-Suns while solar cell temperature

ranged from –110 to 25 °C. Figures 17a and 17b show Isc test results of a grade 8 solar cell (#3055) under LILT conditions with the VCL light source. Over the full range of temperatures and illumination levels, the Isc response is well behaved: that is, the magnitude of Isc is proportional to the illumination intensity and Isc increases monotonically with increasing temperature.

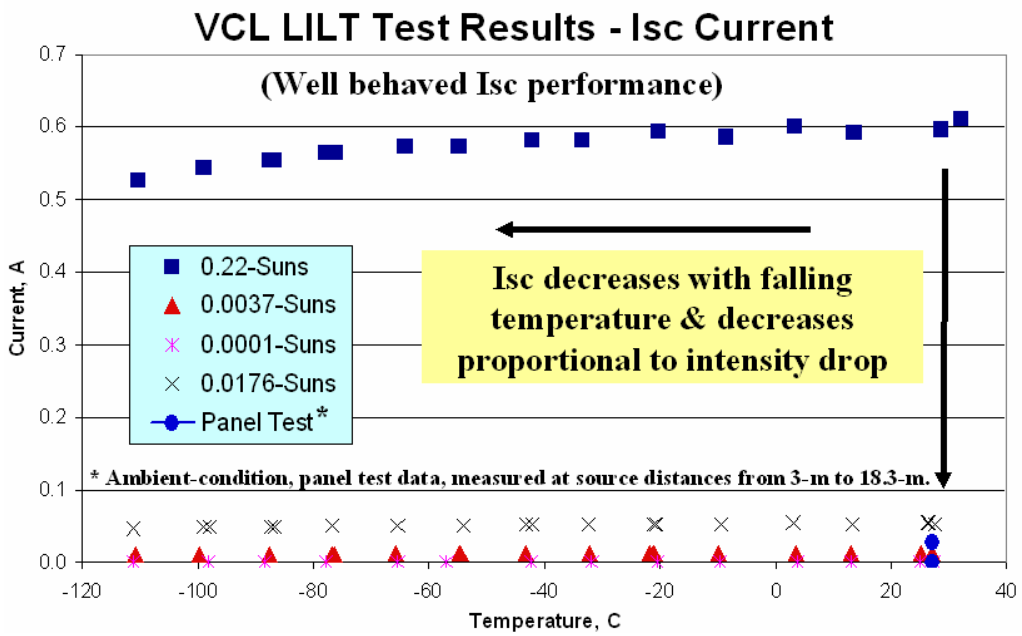

Figure 17a.—ISS solar cell Isc – VCL LILT conditions.

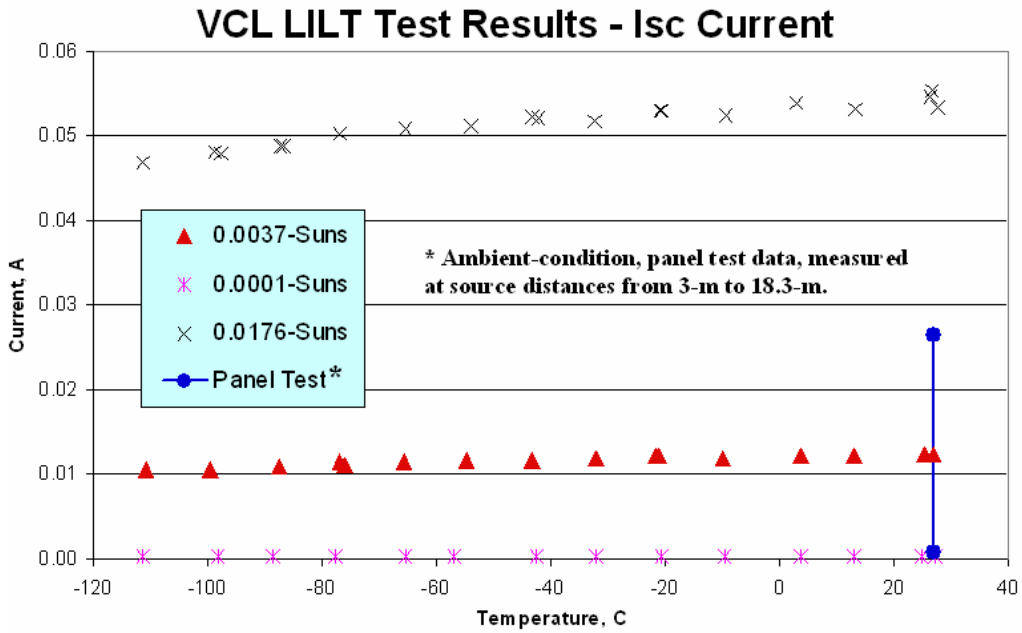

Figure 17b.—ISS solar cell Isc – VCL LILT conditions (reduced current scale).

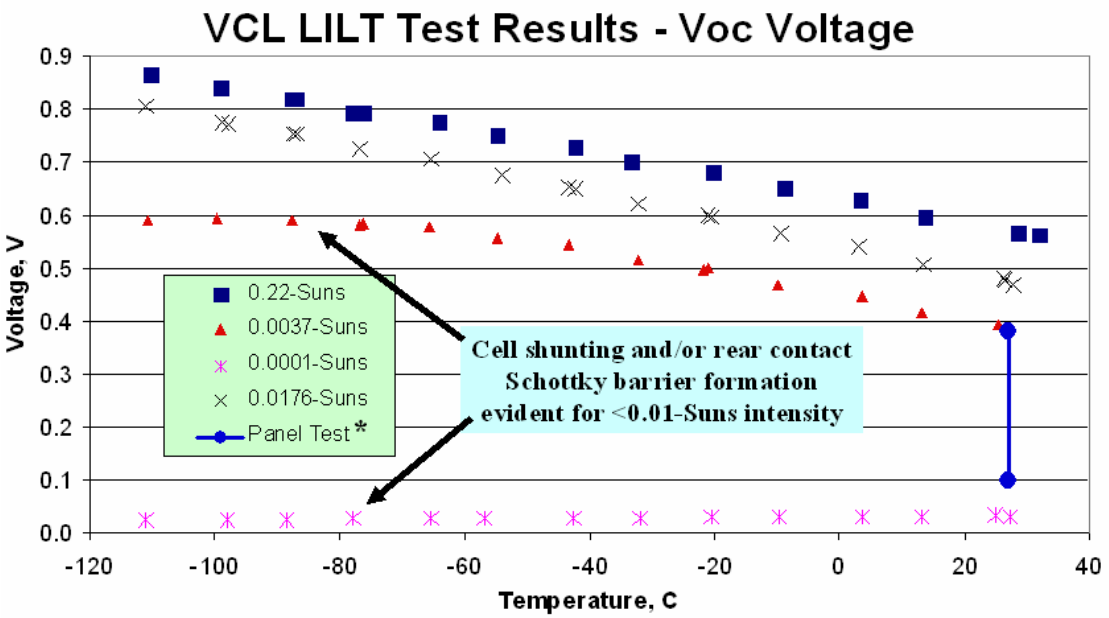

Figure 18.—ISS solar cell Voc—VCL LILT conditions (*Ambient-condition, per-cell, panel test data, measured at source distances from 3-m to 18.3-m.)

Figure 18 shows Voc test results of a grade 8 solar cell (#3055) under LILT conditions with the VCL light source. Over a wide range of temperatures and illumination levels, the Voc response is well behaved: the magnitude of Voc varies with the natural logarithm of intensity and Voc decreases monotonically with increasing temperature level. However, LILT shunting and Schottky loss mechanisms are apparent at 0.0037-Suns intensity for temperatures below ~–60 °C (flattening of the Voc versus temperature slope) and over the full temperature range at 0.0001-Suns intensity (Voc actually increases ~33 percent with increasing temperature over the range of –110 to 25 °C).

Solar cell LILT data with a VCL light source suggests that, for a low illumination level (0.0001-Suns), maximum string Voc and Isc capability during eclipse lighting scenarios will occur at warmer temperatures.

4.4 VCL/Ambient Panel

A grade 7, 80-cell panel (PPM #1083 – same panel used for full moon testing) was positioned at various distances from the VCL light source and at each position, the panel current-voltage curve was measured. Tests were conducted in a lab under ambient conditions with an estimated temperature of 27 °C. Isc and Voc data are illustrated with triangle and circle symbols in Figures 19a and 19b, respectively. Uncorrected and corrected data are shown. The data was corrected to subtract the current and voltage contributions from spurious lighting and reflections. The corrected data were also fit to power-law functions to allow extrapolation of results to greater distances.

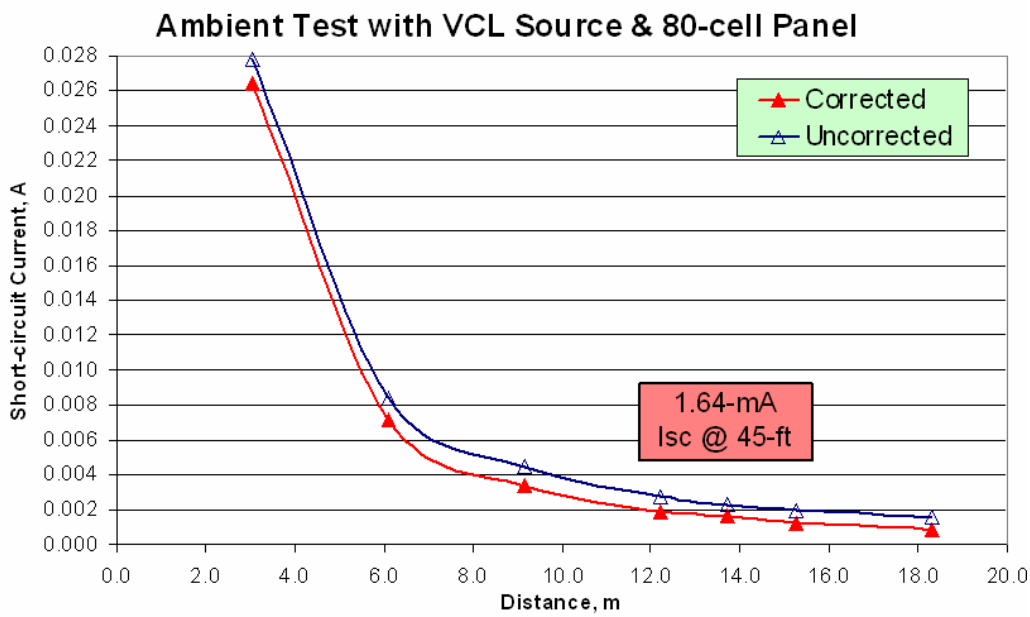

Figure 19a.—80-cell panel (PPM) Isc versus distance—ambient testing with VCL

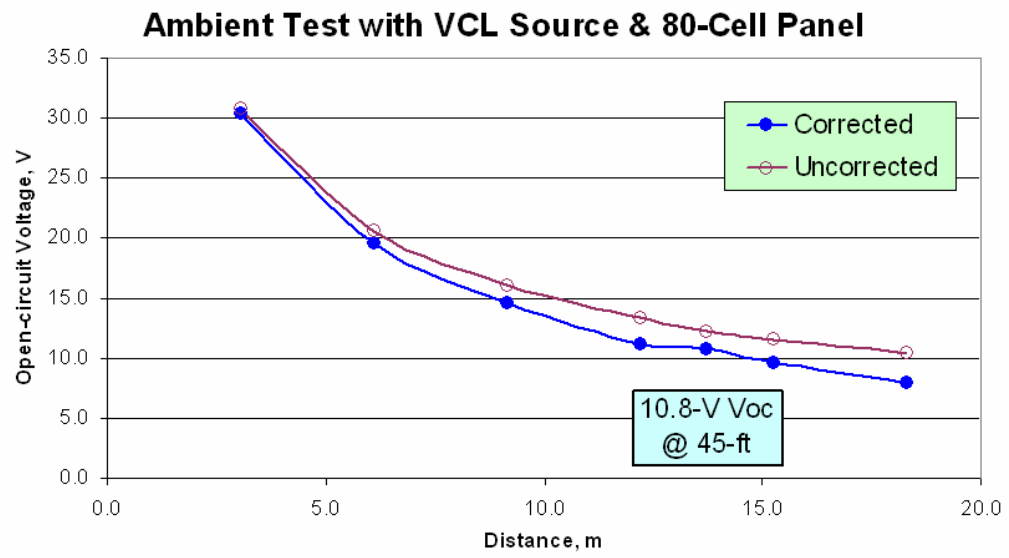

Figure 19b.—80-cell panel (PPM) Voc versus distance—ambient testing with VCL

Going from a distance of 18 to 3-m, the panel Isc follows the inverse distance squared rule within 10 percent up to a distance of 6-m. At a 3-m distance, Isc is 17 percent lower than would be calculated by scaling results with the inverse distance squared rule. The likely reason for this is discussed in the next section below.

At a 13.7-m (45-ft) distance, typical of the distance between a post-15A ISS truss VCL and an in-board SAW, the measured Isc is 0.00164-amps while the Voc is 10.8-volts for the 80-cell panel. A simple scaling of these data suggest that a 400-cell ISS SAW string could have a current capacity greater than 1-mA and voltage capability greater than 50-volts: both of these values exceed the safety limits defined for EVA crew members.

4.5 Comparison of Solar Cell and Panel VCL Test Results

For comparison purposes, the 80-cell panel test results are plotted on the same graphs used to plot the single solar cell data (Figs. 17b and 18). At the 3-m panel test distance, the per-cell panel Voc and the single cell Voc measurements closely match at a value of 0.39-volts. However, when Isc values are compared, the panel Isc measurement is ~2.5 times higher than that from the single cell test. The illumination intensity for the single cell tests was estimated as 0.0037-Suns while that estimated for the panel test at 3-m distance was 0.0048-Suns +26/–17 percent (scaling the VCL lumen data based on the inverse distance squared rule and applying the lumens to solar cell correction factor of 2 times). Thus, the estimated illumination levels are roughly within 25 percent of each other; not enough to explain a factor of 2.5 times difference in current.

Although a definitive explanation for the cause of this 2.5 times difference in measured current levels for the same Voc value is not in hand, there are two likely contributing causes. The first likely cause is large short-range, VCL beam flux non-uniformity over the PPM panel area. This is illustrated in Figure 20 showing VCL target plane flux variations over the panel area at 18.3-m (60-ft) {shown in yellow highlight} and at 3-m (10-ft) {shown as heavy black border}.

The estimated flux variation over the panel area increases from 11 percent at 18.3-m to 46 percent at 3-m distance. Under short-circuit conditions, weakly illuminated solar cells in the panel are driven to reverse-bias. At this point, by-pass diodes turn-on in forward conducting mode and effectively eliminate affected 10-cell submodules in lowest flux regions from the panel circuit. The remaining 10-cell submodule(s) in the highest flux regions then drive the higher measured Isc value. By-pass diodes can conduct VCL-illuminated Isc current levels (0.027-amps) with low forward voltage drop (0.4-volts). This voltage drop is easily made up by the active cells in the string resulting in only a very small solar cell current loss. Due to the high solar cell shunt resistance, the current leg of current-voltage curve is flat (see Figure 14a) so that cells can operate at a small to moderate voltage level with little loss in current.

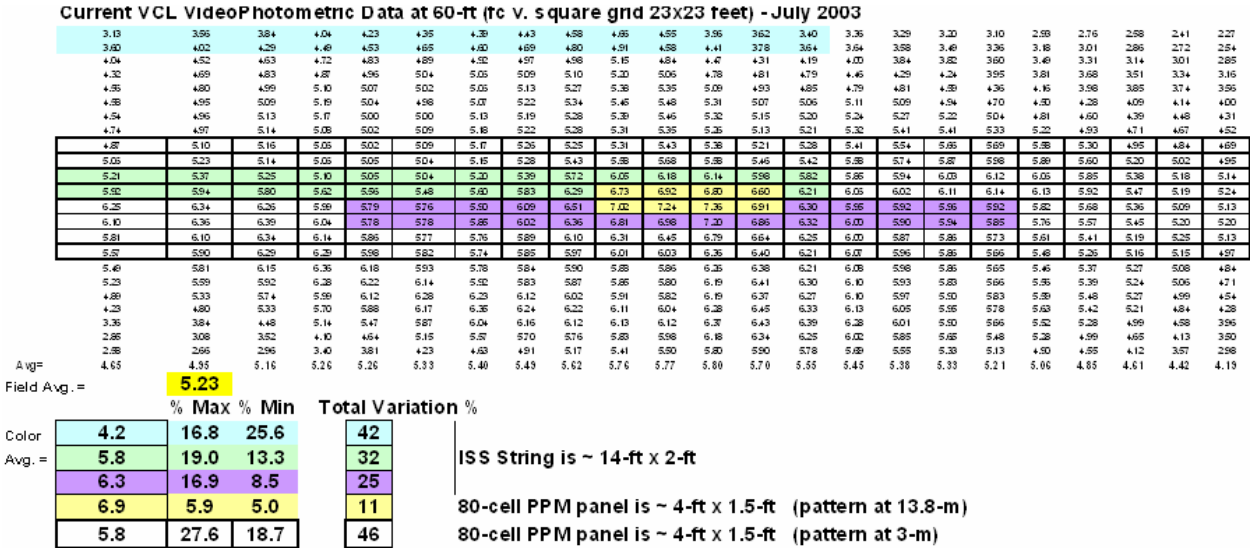

Figure 20.—Flux uniformity of VCL beam of ISS string area and 80-cell test panel area.

For example, in the limiting case of only one active 10-cell submodule (and 7 active by-pass diodes), the voltage drop in the multiple by-pass diodes would be 2.8-volts. Divided among the 10 active cells, each cell must operate at a 0.28-volt voltage. The current at this voltage is 99.6 percent that of Isc (essentially equal to Isc). Thus, it is conceivable that the panel testing a short range with high non-uniformity was measuring the current level produced by only one 10-cell grouping in the highest flux region. The actual VCL flux distribution at 3-m distance has not been measured. Thus, the VCL illumination non-uniformity could be, and is likely, much higher than the estimated 46 percent based on the measurement at 18.3-m distance on a 0.3-m by 0.3-m square grid field. One contributor to enhanced illumination non-uniformity at short range would be the diffusely reflecting band around the front face of the VCL. This higher non-uniformity, coupled with the panel by-pass diode and solar cell properties, could explain a 2.5 times current difference measured in panel versus single solar cell tests. For the Voc measurement, the panel current level is zero and by-pass diodes are not a factor. Panel individual solar cell Voc values will vary weakly with local illumination level, but will all add up in the series-connected panel to provide a panel Voc indicative of the average illumination level over the entire panel.

The second likely cause of this 2.5 times difference in measured current levels for the same Voc value is non-proportionality of solar cell current-voltage performance with illumination intensity at low intensity levels. For these tests, illumination intensity is estimated based on the measured solar cell Isc. The illumination intensity, in Suns, is assumed to be proportional to the ratio of Isc measured to Isc measured at a calibrated 1-Sun intensity. Similarly, the solar cell Voc is assumed to be proportional to $\ln(Isc/I_o)$ where I_o is the diode saturation current. However, at low intensity, cell shunt currents become relatively large and degrade cell current and voltage output. The threshold intensity, below which the cell departs from proportional current-voltage behavior versus illumination intensity, was not measured. Yet, this threshold illumination intensity value is a function of the cell quality (cell grade) as indicated by LILT test data. These data showed that grade 5 cells had poorer Isc, Voc and fill factors at low illumination intensities (relative to 1-Sun intensity) when compared to those of grade 8 cells. Hence, different current-voltage performance can be expected from a grade 8 cell compared to a panel with grade-7 cells.

4.6 Solar Cell and VCL Spectral Characteristics

The measured ISS silicon solar cell spectral response is shown in Figure 21. The solar cell was mounted on the Kapton-glass scrim cloth flexible panel lay-up. This shows up in the backside data as a loss in overall response in addition to preferential blue loss. Integrating the data sets shows that the average front side response in the near infrared (700 to 1000 nm) is 31 percent greater than that of the visible (400 to 700 nm). Also, the integrated backside response is 44 percent that of the front side and is consistent with the 41 percent value from past solar cell front side and backside Isc measurements (Ref. 19).

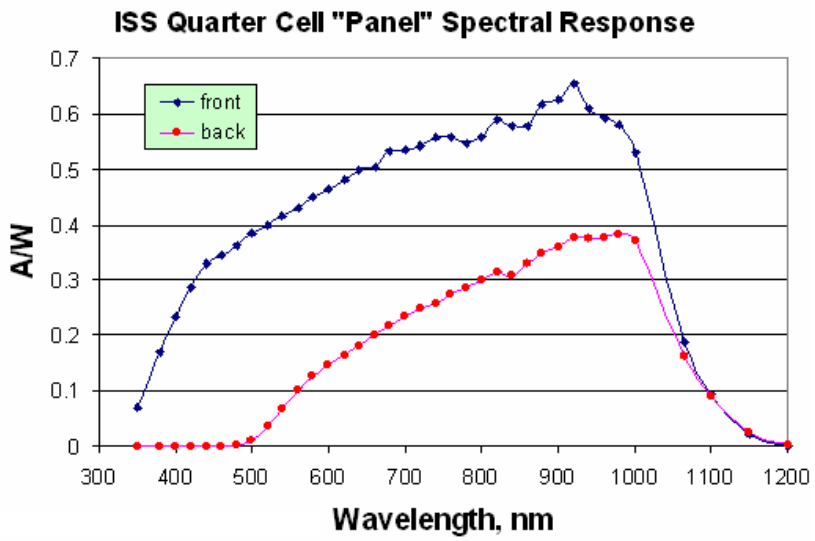

Figure 21.—Measured ISS solar cell spectral response.

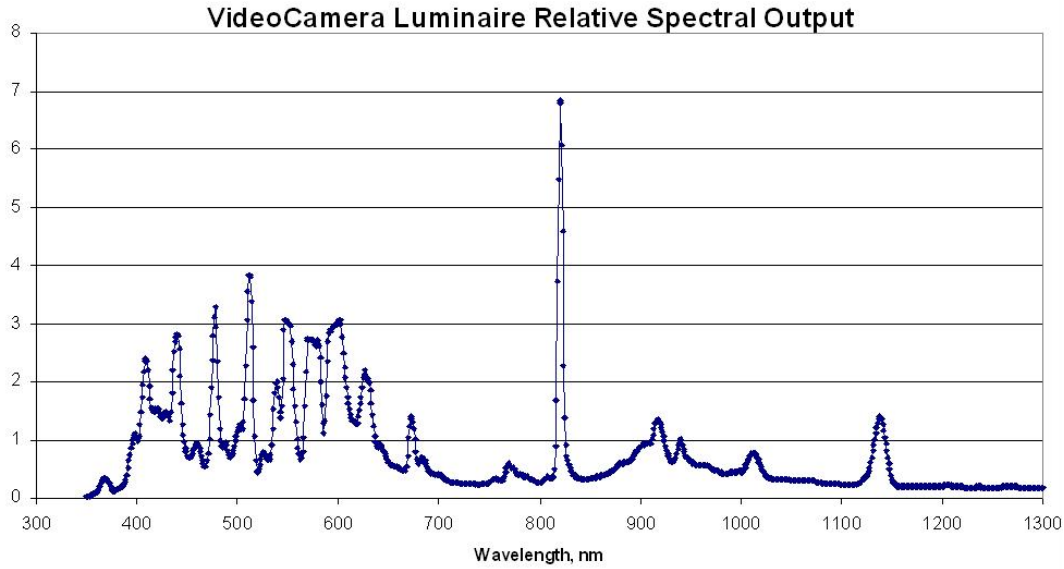

Figure 22.—Measured VCL relative spectral irradiance.

The VCL was operated at 120-volts DC and 1.56-amps for a period of 4-hours. At this point, the VCL relative spectral irradiance was measured and is shown in Figure 22. Integrating these spectral irradiance data shows that ~50 percent of the energy output is in the visible band (400 to 700 nm) while ~75 percent of the output is within the band response of the ISS silicon solar cells (400 to 1100 nm). Since the solar cells have a ~30 percent stronger response in the near infrared when compared to the visible, one can expect the solar cell current output to be ~2.0 times higher than the current associated with the VCL lumen output (intensity tied to the visible band energy only). Therefore, for this worst case assessment, we assume that the effective VCL intensity is 2 times that indicated by the lumen output.

5.0 Orbital Eclipse Lighting Assessment

The goal of this eclipse lighting assessment is to calculate the highest possible values of illumination intensity on ISS solar array blankets under all credible lighting scenarios. These highest illumination conditions will lead to the greatest calculated values for SAW string current and voltage capacity; hence, the "worst-case" situation from the standpoint of electrical hazards. *Nominal orbital eclipse lighting conditions will lead to reduced SAW string electrical hazard levels*. However, to assess nominal electrical hazards, specific operational information is required such as the exact location of EVA crew members (i.e., EVA helmet light position) and the exact alpha gimbal and/or SAW beta gimbal park angles (i.e., impact on VCL and full moon incidence angles). All of the required specific information is not yet available, so this assessment will only include "best-case" lighting scenarios (worst-case SAW electrical hazards).

5.1 Natural Lighting (Full Moon)

The average full moon light intensity in low Earth orbit, 0.00235 W/m^2 (1.70×10^{-6} Suns), was estimated by taking the product of equinox solar insolation (1 Sun = 1371 W/m^2), visual geometric albedo at 5 percent phase angle (0.084) and the square of the quotient of lunar equatorial radius (1737.4 km) and mean Earth-moon separation distance (384467 km). The maximum full moon light intensity in low Earth orbit is 0.00282 W/m^2 (2.06×10^{-6} Suns) accounting for maximum solar insolation (1418 W/m^2) and minimum lunar separation (356922 km). This is the maximum full moon illumination intensity possible assuming the SAW blanket front side surface normal is aligned with the moon position vector, i.e. no cosine pointing loss.

5.2 Artificial Lighting

Colleagues from The Boeing Company, Mr. David Karakula and Mr. David Moore, provided ISS artificial lighting information in emails and faxes sent in July 2003 and May 2004, respectively. This information included the types of lighting on ISS (CETA lamps and VCLs) and on EMUs (helmet lights), the positions or likely positions of these light sources, the ability to pan light sources in various directions, light source operating specifications (i.e., power consumption, etc.), and illumination intensity data (VCLs). Based on this information and other information and assumptions by the authors, *hand calculations were performed* to estimate light source intensity on SAWs based on:

(1) scaling dimensioned drawings and,
(2) *assuming* that light source intensity level decreased proportionally with the inverse square of distance from the light source (true for Lambertian sources and approximately true for sources with divergent optics). This assumption is accurate within 10 percent for the VCL light source based on PPM current data measured at distances from 6 to 18-m from the source.

All of these preliminary assessments were performed for the best-case lighting scenario (best-case SAW string electrical performance) which gives the "worst-case" electrical hazard scenario. This means that the light sources nearest to the SAWs and panned in a direction to the nearest portion of the SAW blankets were assessed. For the SAW being assessed, the ISS alpha gimbal (if present) and SAW beta gimbal were assumed to be at angles that maximized the incident light intensity on the SAW blanket front side factoring in cosine loss and inverse square of distance rules.

5.2.1 CETA lamps

Crew/Equipment Translation Aid (CETA) lamps illuminate EVA crew and cart translation corridors on ISS. CETA lamps are fixed luminaires and can not be re-directed. They point towards the center truss segment S0, the CETA cart and the "Quest" airlock. As such, these lamps are not directed toward SAWs currently located on the Z1 truss segment or future SAW positions outboard of truss segments P3/S3. Thus, CETA lamps were excluded from this eclipse artificial lighting assessment.

5.2.2 EMU helmet lighting

Extravehicular Mobility Unit (EMU) helmet lights are shown in Figure 2. Each helmet has a pair (one left, one right) of flood lights and a pair of spot lights. Each light has a 6-watt Halogen cycle tungsten filament bulb. Crew members can activate a 3-position toggle switch (one on the helmet right side and one on the left side) to turn on the flood light or turn on the spot light or turn all lights off. Thus, a maximum of two lights can be operational per EMU. With 2 flood lights operating (left and right), a "wide-area," 0.66-m diameter spot is illuminated at a 0.61-m distance with 15 foot-candle average intensity and a spatial uniformity of ±33 percent. With 2 spot lights operating (left and right), a "tight beam," 0.46-m diameter spot is illuminated at 3-m range with a 9 foot-candle average intensity and a spatial uniformity of ±11 percent. For reference, a foot-candle of light is based on the sensitivity of the human eye. At a 555-nm wavelength (green), it is equal to approximately 0.0157 W/m^2. The helmet light filament color temperature and spectral output was not specified. Typical tungsten halogen lamp relative spectral output curves are shown in Figure 23. Lastly, the helmet lights can point in any direction as the EVA crew member has the ability to face in any direction.

For any EVA, including an SSU R&R, two EVA crew members are required: EV1 and EV2. EV1 will be working close to the SSU (Fig. 24) while the location of EV2 is uncertain at this time. Presumably, EV2 will be within line-of-sight with EV1 and located in or near a CETA ingress/egress corridor near the truss elements. Thus, the greatest illumination from EV1 helmet lights will occur on either SAW blanket backside and at the base solar cell string (closest to mast canister).

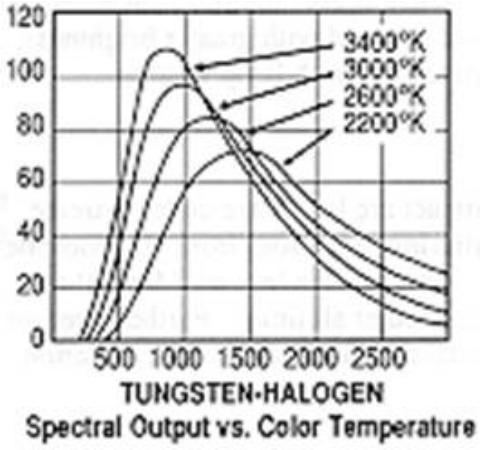

Figure 23.—Relative spectral output versus wavelength (nm) and filament color temperature (K).

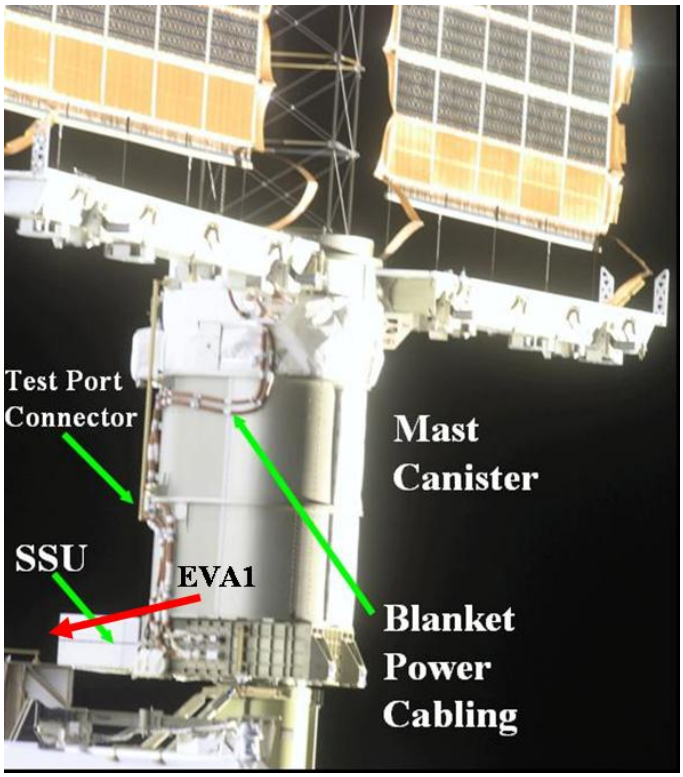

Figure 24.—Configuration of SSU and SAW.

Located near the SSU, EV1 helmet light-to-base-string distance is approximately 3.8-m and the light strikes the SAW blanket backside at approximately a 78° incidence angle. In flood light mode, a helmet light pair yields a 4.1-m diameter illumination area per EVA crew member. This is just large enough to fully illuminate a single SAW string. Since the position of EV2 is unknown, it is assumed that EV2 produces similar SAW illumination as EV1 and the illumination fluxes are additive over same SAW string area (i.e., both crew members looking at the same string). A beam intensity reduction factor of 0.2 is applied for cosine loss and 0.67 is applied consistent with the ±33 percent non-uniformity in beam illumination. It is also assumed that the light luminous output is ~2 times greater than light foot-candle rating (tied to the response of the human eye). This accounts for the integrated spectral response of a silicon solar cell (from 400 to 1100 nm) that is ~2 times greater than that of a human eye (over 400 to 700 nm). Lastly, a beam intensity reduction factor of 0.41 is applied to account for backside SAW illumination that produces only 41 percent of the current compared to front side illumination (Ref. 19). Thus, the resulting equivalent illumination intensity on the front side of the SAW base string is 8.7×10^{-7} Suns (for two EVA crew members both with a pair of flood lights operating).

In spot light mode, a helmet light pair yields only a 0.57-m diameter illumination area per EVA crew member. This would illuminate only ~1/8th of the area of a full solar cell string per crew member or about 1/4th the area of a full string with spot mode illumination from 2 EMUs. As such, the string Voc would be 4 times less than a fully illuminated string. Also, the string Isc (produced by illuminated cells) would be current-limited by the ~38 series by-pass diodes (one for each 8 solar cells) that must forward conduct the string current for non-illuminated cells. Due to these string performance limiters, the EMU helmet spot light mode illumination case was excluded from further assessment.

5.2.3 VCL Lighting

Video Camera Luminaires or VCLs (see Fig. 1 for nomenclature and locations) are not fixed, but instead can be pointed in any direction. For this best-case lighting assessment, VCLs were assumed to point in direction to maximize SAW illumination intensity. For the present ISS-11A configuration (or any configuration with SAWs on the Z1 truss), the S1-CP3 VCL does not have full view of SAW 2B (closer wing) or SAW 4B (further wing) due to S1 truss blockage. The VCL beam could, however, illuminate the outer edge of the –X blankets of these wings (Fig. 25). Thus, CP3 VCL illumination cases were eliminated from the ISS-11A assessment.

The Lab-CP13 VCL can illuminate both SAW 2B and 4B although the 2B can be best illuminated. The greatest illumination case occurs for a specific beta gimbal angle that fully illuminates the 2B, +X blanket with normal incidence in the ISS XZ plane. For this case, the SAW base string distance from the CP13 VCL is ~23-m (75.4-ft) and the ISS XY plane

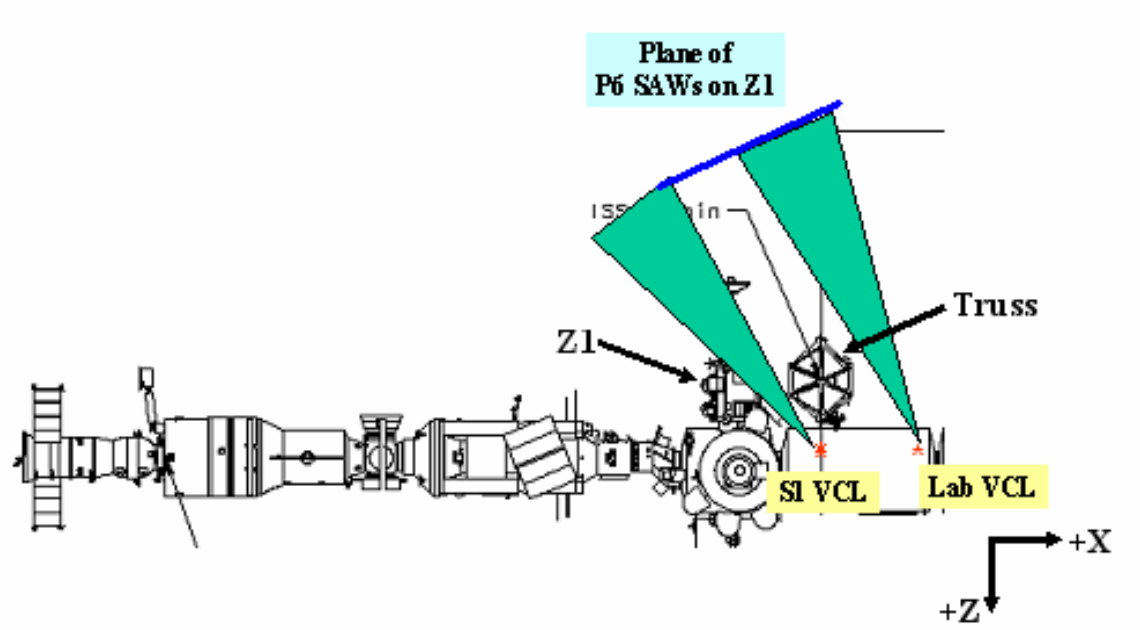

Figure 25.—Approximate VCL light beams on ISS-11A, P6 SAWs on the Z1 truss.

incidence angle of the VCL beam on the SAW 2B is ~25°. The equivalent illumination intensity is 6.2×10^{-5} Suns. This value was determined by: (1) scaling the VCL lumens intensity data (Fig. 9a) with inverse distance squared, (2) applying a beam uniformity reduction factor of 0.88 consistent with the VCL illumination spatial uniformity of ±12 percent at 23-m, (3) applying a beam intensity reduction factor of cosine (25°) and (4) applying a beam intensity factor of 2 times (based on the VCL spectrum discussion in section 4.6) to account for the enhanced spectral response of a silicon solar cell over the human eye (lumens adjustment). The corresponding beam spot size would allow for ~5 strings to be fully illuminated.

For ISS post-15A future configurations, there are equal best-case lighting scenarios that include the S1-CP2 or -CP3 VCLs illuminating the in-board S4 SAWs 1A or 3A or the P1-CP8 or -CP9 VCLs illuminating the in-board P4 SAWs 2A or 4A. Figure 26 shows an example configuration with a P1 VCL illuminating a P4 SAW. The greatest illumination level will occur when: (1) the alpha gimbal position places the SAW along the ISS Z-axis and (2) the VCL is directed at the base SAW string (nearest to mast canister). The maximum (worst-case) string current will be possible when the in-board SAW front side faces in-board toward the VCL. In addition, VCL illumination intensity on the SAW is a function of function of beta gimbal position which affects SAW-VCL distance and beam incidence angle on the SAW. Beam intensity is maximized when the SAW +X blanket is 23° off the X-axis. The corresponding VCL to SAW distance is ~12.6-m (41.3-ft) and VCL beam incidence angle on the SAW is ~28°. Under these illumination conditions, the equivalent illumination intensity, including all scaling and intensity factor adjustments, is 2.0×10^{-4} Suns. The beam spot size allows for only a single string to be fully illuminated.

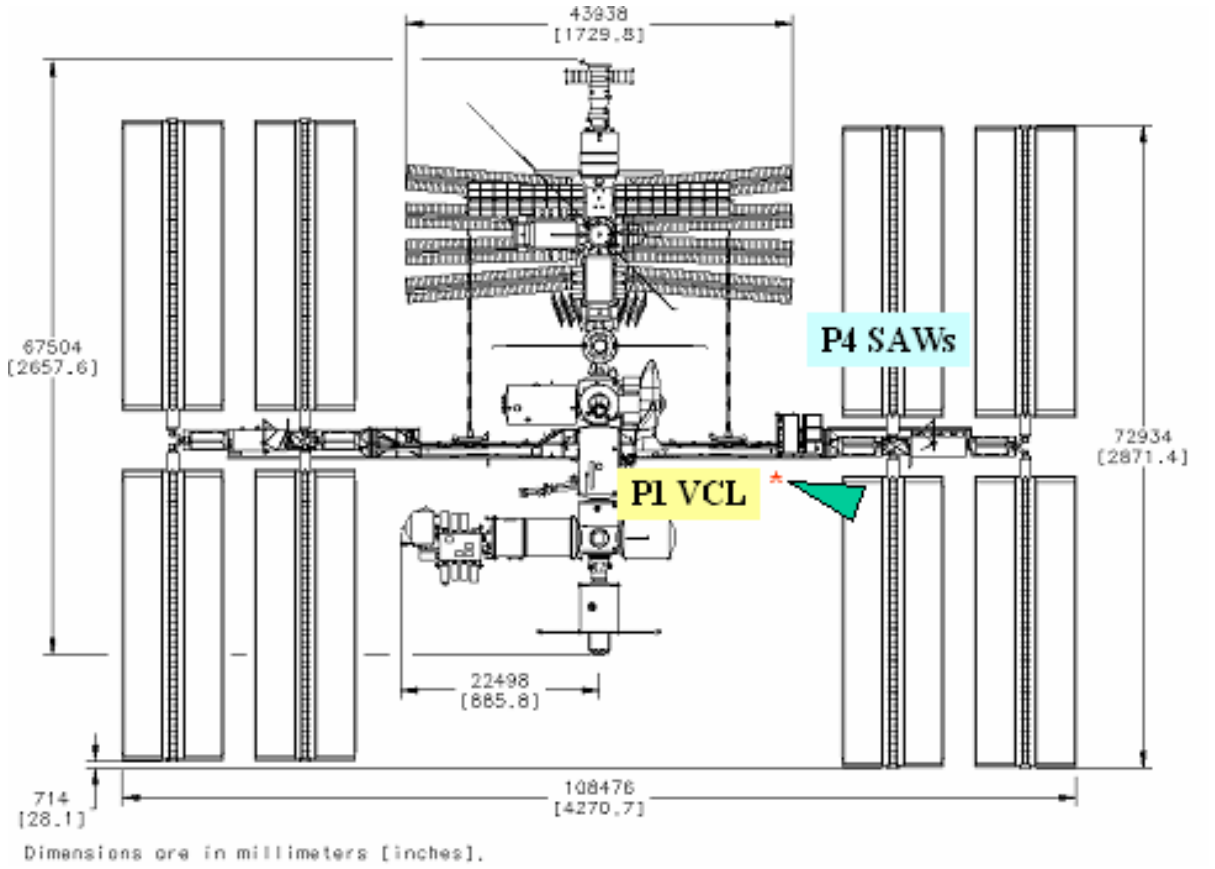

Figure 26.—Approximate P1 VCL light beam on ISS-15A+, P4 SAWs.

5.3 Reflections

It is feasible that light source illumination could be reflected from ISS surfaces and/or docked orbital vehicle surfaces such as the US space shuttle orbiter, the Russian Soyuz/Progress vehicles, the European Automated Transfer Vehicle (ATV) and the Japanese H-II Transfer Vehicle (HTV). Most surfaces reflect light either diffusely (reflected in all directions) or specularly (reflected in opposite direction with equal incoming and outgoing incidence). Most ISS and orbital vehicle surfaces are designed to be diffuse for improved thermal control and to minimize sunlight glint that could affect the operation of star trackers and sun position sensors or hinder crew member viewing.

The exception to this practice is photovoltaic arrays: that is, the active array surface is populated with solar cells covered with glass slides which, in turn, are coated with multiple dielectric filter layers (photovoltaic array inactive side, i.e., back side, is diffuse). The filter layers are optically smooth and behave as specular reflectors. The filters are designed to absorb useful photons (visible), reject sub-bandgap photons (infrared (IR)) and reflect highly energetic, damaging photons (ultraviolet (UV)). Sub-bandgap IR light reflections are not relevant to this assessment since they can not produce a photovoltaic effect. The UV (<350 nm) component of incident light is very small since none is produced by the VCL and EMU helmet lights (Figs. 22 and 23) and the small fraction of UV in the AM0 spectrum (about 4 percent; see Fig. 8b) is not well reflected by the moon (albedo of about 0.05; see Fig. 7). Thus, photovoltaic arrays will not

reflect much UV light (about 45 percent of the incident full moon UV light intensity). Finally, the dielectric filter stack effectively absorbs most of the useful, in-band light reflecting only 10 to 15 percent in a specular fashion.

Diffuse ISS surfaces are comprised mainly of anodized aluminum (moderate solar reflectance of ~0.5) and white thermal control surfaces, such as beta cloth, with a high solar reflectance of about ~0.8. The magnitude of light reflected from one diffuse surface and incident on another surface is proportional to the product of reflecting surface reflectance, inverse of the cosine of incidence angle on the reflecting surface, inverse of the cosine of incidence angle on the receiving surface and inverse of the square of the distance between reflecting and receiving surfaces. Thus, to estimate the magnitude of reflected energy, one needs to ascertain these elements for each type of reflection scenario.

There are two reflection scenarios: reflection from the primary light source and reflections from a secondary light source (further away from, and perhaps with an obstructed view of, the solar array under consideration). There are four sources of light identified for study in this assessment: full moon, CETA lamps, EMU helmet lights, and VCLs. Table 3 contains a representative listing of the most significant reflection source(s) (i.e., those with large area and good view angle to the array) for each type of reflection and for each source. Input data are estimated in most cases and the best-case primary light source and solar array configurations, from the preceding sections, are assumed (i.e., for moonlight, the array front surface normal is assumed to be pointed at the moon).

These results show that all reflections, excepting specular moon light reflection from a SAW front surface, have intensities 0.1 percent or below that of the light source strength and thus, add only a small amount of light on to the SAWs. For full moon illumination cases, a few percent increase in light intensity could occur from reflected moon light. But this will only occur for the unlikely configuration that would allow one SAW to reflect light on to its companion SAW (without at the same time shadowing it).

Table 3.—Inputs and Estimated Magnitudes of Reflected Light on to SAWs

Light Source	Primary or Secondary Reflection Source?	Reflecting Surface	Surface Diffuse or Specular?	Approx. Visible Reflectance	Reflecting Surface Outgoing Angle, deg	SAW Incoming Angle,deg	Approx. Source to Surface* Distance, m	Approx. Surface to SAW* Distance, m	Reflection, % of source Strength
Moon	primary	11A - none							
		15A companian SAW front	specular	0.10	75	15	1	1	2.500
		15A companian SAW back	diffuse	0.45	75	15	1	15	0.050
		15A CTCS radiator	diffuse	0.85	75	15	1	15	0.094
	secondary	11A - none							
		15A companian SAW front	specular	0.10	45	45	1	1	5.000
		15A companian SAW back	diffuse	0.45	45	45	1	15	0.100
		15A CTCS radiator	diffuse	0.85	45	45	1	19	0.118
CETA	primary	11A,15A - none							
	secondary	11A - S0 truss beta cloth	diffuse	0.80	75	30	10	10	0.002
		15A - S0 truss beta cloth	diffuse	0.80	75	30	10	30	0.000
EMU Helmet Light	primary	11A,15A - lower blanket box	diffuse	0.50	70	80	2	1.5	0.330
		11A,15A - mast canister	diffuse	0.50	45	85	1.5	2.5	0.219
	secondary	11A, 15A - P6 beta cloth	diffuse	0.80	55	55	4	6	0.046
		15A - PVTCS radiator	diffuse	0.85	55	55	5	7	0.023
		15A companian SAW front	specular	0.10	5	5	15	1	0.044
		15A companian SAW back	diffuse	0.45	5	5	15	15	0.001
VCL	primary	11A - CP3 none							
		11A - CP13 to P6 beta cloth	diffuse	0.80	30	70	15	6	0.003
		15A - CP3 to S4 beta cloth	diffuse	0.80	70	70	10	5	0.004
		15A - CP3 to S4 Radiator	diffuse	0.85	70	70	12	8	0.001
		15A - CP3 to S4 SAW front	specular	0.10	75	15	10	1	0.025
		15A - CP3 to S4 SAW back	diffuse	0.45	75	15	10	15	0.001
	secondary	11A - CP3 to Lab	diffuse	0.50	30	30	20	15	0.000

*** - A value of "1" implies no correction for distance.**

Given the small intensity of reflected light for a variety of representative lighting scenarios, we conclude that it is a reasonable assumption to ignore the contribution of reflected light in assessing SAW LILT performance.

5.4 Combined Lighting Effects and Equivalent Lighting Intensity Results

Although unlikely, it is also feasible that a single solar array string could be simultaneously illuminated by full moon light, VCL lighting, EMU helmet lighting and reflected light sources. As discussed above, light source reflections can be ignored. The equivalent intensity of these light sources individually and combined is shown in Table 4.

Table 4.—Equivalent Light Intensities on the SAW

Eclipse Illumination Case	Greatest Possible Equivalent SAW Front Side Illumination Intensity (Suns)
Full Moon	2.06×10^{-6}
EMU Helmet Flood Lights	8.70×10^{-7}
VCL – ISS 11A*	6.20×10^{-5}
VCL – ISS 15A**	2.00×10^{-4}
Combined – Full Moon + Helmet Lights	2.93×10^{-6}
Combined – Full Moon + VCL 11A[1]	6.29×10^{-5}
Combined – Full Moon + VCL 15A[2]	2.01×10^{-4}
Combined – Full Moon + Helmet Lights + VCL 11A[1]	6.49×10^{-5}
Combined – Full Moon + Helmet Lights + VCL 15A[1]	2.03×10^{-4}

[1]Or any ISS configuration with SAWs on Z1.
[2]Or any ISS configuration with SAWs on S4/P4.

6.0 Solar Array Electrical Performance Results

The lighting assessment above fixes the effective illumination levels (Table 4) used to assess solar array wing string electrical performance, but does not address the proper operating temperature to consider. Figure 27 below shows calculated sun-tracking array string temperatures versus orbit time for several values of solar beta angle. The coldest solar cell temperature during eclipse, ~–80 °C, occurs just before eclipse exit for a 0° beta orbit. Temperatures in this range will exist for many minutes as temperature transients are mild. The warmest solar cell temperature during eclipse, ~+40 °C, occurs just after eclipse entrance for a 25° beta orbit. Due to the high temperature transient upon entering eclipse, solar cell temperature will stay in the warm range for much less than 1-minute. For this worst-case assessment, LILT Voc values will be evaluated +40 °C while LILT Isc values will be evaluated at –80 °C.

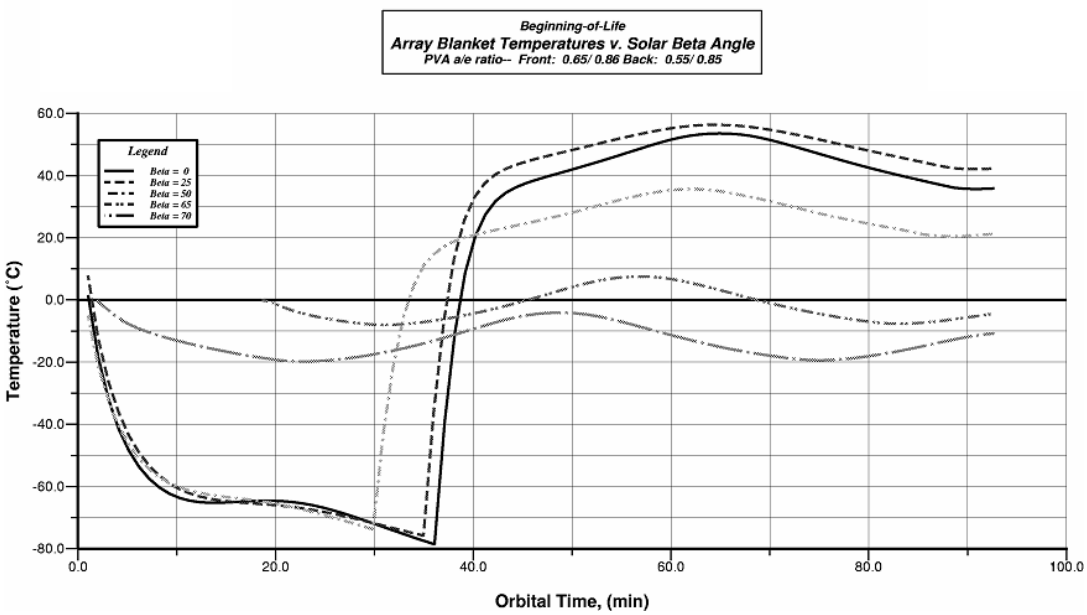

Figure 27.—Calculated SAW string operating temperatures.

6.1 Full Moon

The uncorrected panel I-V data (from Figure 13) were adjusted as follows: (1) remove spurious, ambient light contribution in test data (added 10 percent to current), (2) scale 80-cell test results to 400-cell string configuration by multiplying voltage values by 5, (3) apply orbital operating temperature (+40/–80 °C for best performance under LILT conditions) correction factors to Isc (factor = 1.148) and Voc (factor = 1.06) data values obtained at 10 °C, (4) scale current data based on ratio of integrated AM0 reflected lunar light intensity to that of the ground test lunar light intensity (Table 1), and (5) apply multiplying factor of 1.1 to currents to account for moonlight reflections off Earth to the backside of the solar array (factor = 1 + Earth albedo × Earth view factor × Solar cell backside to front side ratio of integrated spectral response = 1 + 0.3×0.8×0.4 = 1.1). Applying all these adjustment to the data, one can estimate the best Earth orbiting SAW string operating values of Isc = 11.0×10^{-6}-amps and Voc = 5.5-volts.

6.2 Helmet Lights

The EMU helmet lights produce very weak lighting, 8.70×10^{-7}-Suns, on the SAW base string. This intensity level is far below that tested in the laboratory and about half the intensity of the full moon. Two approaches for estimating string Isc and Voc were explored. Both methods applied temperature corrections to Isc and Voc data. Method one scaled down the full moon data with illumination intensity to get estimates of Isc = 4.8×10^{-6}-amps and Voc = 4.9-volts. Method 2 scaled down single cell data obtained at 0.00047-Suns X-25 illumination and resulted in estimates of Isc = 5.0×10^{-6}-amps and Voc = 2.9-volts. The Isc estimates of both methods give a close answer, 5.0×10^{-6}-amps, while the Voc answers are different, but both below 5-volts (a safe voltage level).

6.3 VCLs

Single cell data obtained at 0.00047-Suns X-25 illumination were scaled down to the VCL lighting case flux levels and temperature corrected to obtain estimates for SAW string Isc = 0.00033-amps and Voc = 0.94-volts for ISS-11A and Isc= 0.00108-amps and Voc = 3.35-volts for post ISS-15A.

Similarly, single cell data obtained at 0.0001-Suns VCL illumination were scaled up or down to the VCL lighting case flux levels and temperature corrected to obtain estimates for SAW string Isc = 0.00025-amps and Voc = 4.4-volts for ISS-11A and Isc= 0.00082-amps and Voc = 25.8-volts for post ISS-15A.

In addition to illumination level and temperature corrections, the 80-cell PPM panel Isc data must be corrected for ISS SAW string application to account for the variation in flux over the PPM panel area (–5 percent) versus that over an ISS SAW string area (–8.5 pecent). This flux variation is an indicator of solar cell circuit current limiting behavior. The correction factor at 18.3-m is given by (1-0.085)/(1-0.05) = 0.963. The resulting estimates for the SAW string were Isc = 0.00054-amps and Voc = 33.0-volts for ISS-11A and Isc = 0.00164-amps and Voc = 53.3-volts for post ISS-15A.

The Isc estimates obtained from each of the three data sets agree with each other within a factor of 2. However, the Voc estimates differ by as much as a factor of ~30. We believe that the 80-cell panel derived estimates for Voc have the highest fidelity since the data required the least amount of scaling and corrections compared to the single cell data sets. Direct panel Isc and Voc measurements were obtained with a 1/5th scale panel (80 cells versus 400 cells in a SAW string) at the correct distance from the correct light source. Therefore, for this worst-case (maximum) SAW string performance assessment, we must use the 80-cell panel derived performance estimates.

6.4 Combined Lighting

Although unlikely, it is also feasible that a single solar array string could be simultaneously illuminated by full moon light, VCL lighting, EMU helmet lighting and reflected light sources. Each of these light sources contributes a component of the string total current production (or Isc). Linear superposition of current components to obtain the total string current is permitted due to the linear partial differential equations that describe the diffusion of electrons and holes in the solar cell junction (Ref. 20). Based on a single diode solar cell electrical model (Fig. 4), it can be shown that the Voc of a solar cell (or string) is proportional to ln (Isc/I_o), where I_o is the diode saturation current (Ref. 19). Therefore, string Voc under multi-component illumination can be calculated using ln (Isc/I_o) as a scaling factor, i.e., $Voc_2/Voc_1 = \ln (Isc_2/I_o)/\ln (Isc_1/I_o)$.

Using linear summation of currents and logarithmic scaling of voltage, the calculated values of SAW string Isc and Voc under combined lighting conditions is summarized in Table 5.

Table 5.—SAW String Calculated Performance Under Eclipse Lighting Scenarios
[Highlighted values exceed EVA crew shock hazard limits.]

Eclipse Illumination Case	SAW String Isc (A)	SAW String Voc (V)
Full Moon	11.0×10^{-6}	5.5
EMU Helmet Flood Lights	5.0×10^{-6}	< 5
VCL – ISS 11A[1]		
X-25 Solar Cell LILT Data	0.0003	0.9
VCL Solar Cell LILT Data	0.0002	4.4
VCL Panel Data	0.0005	33.0
VCL – ISS 15A[2]		
X-25 Solar Cell LILT Data	0.0011	3.3
VCL Solar Cell LILT Data	0.0008	25.8
VCL Panel Data	0.0016	53.3
Combined – Full Moon + Helmet Lights	16.0×10^{-6}	5.7
Combined – Full Moon + VCL 11A[1]		
X-25 Solar Cell LILT Data	0.000307	0.9
VCL Solar Cell LILT Data	0.000204	4.7
VCL Panel Data	0.000511	33.4
Combined – Full Moon + VCL 15A[2]		
X-25 Solar Cell LILT Data	0.001108	3.3
VCL Solar Cell LILT Data	0.000806	25.9
VCL Panel Data	0.001611	53.4
Combined – Full Moon + Helmet Lights + VCL 11A[1]		
X-25 Solar Cell LILT Data	0.000310	1.0
VCL Solar Cell LILT Data	0.000206	4.9
VCL Panel Data	0.000516	33.5
Combined – Full Moon + Helmet Lights + VCL 15A[1]		
X-25 Solar Cell LILT Data	0.001111	3.3
VCL Solar Cell LILT Data	0.000808	26.0
VCL Panel Data	0.001616	53.5

[1]Or any ISS configuration with SAWs on Z1.
[2]Or any ISS configuration with SAWs on S4/P4.

The values highlighted in yellow exceed the safe current-voltage levels to avoid human shock (<32-volts, <0.001-amp (Refs. 6, 7, and 10)). All exceedances are associated with VCL illumination scenarios. To reduce these current and voltage levels, controls must be implemented such as deliberate positioning of alpha and/or beta gimbals or deliberate off-pointing of VCLs or powering-down VCLs.

6.5 Discussion of Assessment Uncertainties and Limitations

This preliminary assessment has many inherent uncertainties and certain limitations. Those uncertainties and limitations that have been identified are listed below in Table 6. Many of these items could be sufficiently defined with further, more detailed assessments. As in any engineering endeavor, there are likely several unknown (as yet unidentified) uncertainties that can not be elucidated at this time. A detailed uncertainty analysis has not been performed to evaluate the impacts of these uncertainties on calculated values of SAW string Isc and Voc.

Table 6.—SAW String, Eclipse Lighting Performance Assessment Uncertainties and Limitations

Assessment Area	Uncertainty or Limitation	Value Estimate
Crew Shock Hazards	DC Current and Voltage Thresholds	±100%
Natural & Artificial Lighting	Alpha & Beta Gimbal Positions	±180°
	ISS Geometry, Dimensions and Angles Scaled from Drawings by Hand	±2 m ±10°
	Validity of Inverse Distance Squared Rule for All Light Sources	20%
EMU Helmet Lighting	Spectrum of Lights	***
	Position of EVA Crew Member #1	±2 m
	Position of EVA Crew Member #2	±10 m
	Lighting Effective Pan Angle	4π sr
	Finely Resolved Beam Illumination Distribution at Required Distances	±50%
	Light Intensity Conversion From Lumens to Absolute Engineering Units	±50%
VCL Lighting	VCL Pan Angle	2π sr
	VCL Position	±2 m
	Finely Resolved Beam Illumination Distribution at Required Distances	±50%
	Light Spectral Intensity Conversion From Lumens to Absolute Engineering Units	±50%
	Spectral Intensity of Light in Air Versus Vacuum	<5%
Solar Cell or Panel Performance	Current, Voltage, Flux, Temperature Measurements	<1 to 2%
	Spurious Light Correction for VCL/Panel Testing	25%
	Time After Eclipse Entrance - With Associated Eclipse Operating Temperature of Solar Cell	36 min 120 °C
	Validity of Isc Scaling With Illumination Intensity Under LILT Conditions	±50%
	Validity of Voc Scaling With ln(Isc/I_o) Under LILT Conditions	±100%

7.0 Eclipse Lighting Arcing Assessment

7.1 Solar Array

With the SAW power connectors demated, the string potential will float with respect to ISS and the space plasma. Under illumination, SAW string will generate an open-circuit voltage Voc and the maximum string solar cell voltage difference, ΔV_{max}, will approach Voc. To balance plasma electron and ion collection currents, ~87.5 percent of string solar cells will float negative and 12.5 percent of cells will float positive with respect to plasma neutral (Ref. 21). Thus, for the SAW string, $V_{neg} = -0.875 \times Voc$. SAW string illuminated solar cells with electrical potential act as parallel plate capacitors with the silicon solar cell and plasma (coverglass charge) as the electrodes and the coverglass (thickness δ_1 , dielectric constant κ_1) and coverglass adhesive (δ_2 , κ_2) as the separator. The capacitance, C, of this system is given by $C = 2\varepsilon_o A_c\{\kappa_1\kappa_2/(\kappa_1\delta_2 + \kappa_2\delta_1)\} = \sim 10\ \mu F$, with ε_o as the free space permittivity and A_c as the cell coverglass area

(~21-m^2) discharged by an expanding arc plasma. Here it is assumed that the coverglass charge area swept by the arc plasma is limited to the SAW physical dimensions (blanket width in this case). The discharge arc energy, E, is given by $C*V^2 / 2$, with V as the solar cell voltage which is a linear function $\{0, V_{neg}\}$ distributed over 87.5 percent of solar cells in a string.

A SAW solar cell edge potential must exceed the threshold voltage for a trigger arc to the plasma to occur. Based on two separate SAW string plasma tank tests (Refs. 8 and 9), the trigger arc threshold was determined to be approximately –200-volts. Due to their low energy level, trigger arcs cause no immediately measurable loss in solar cell performance. However, trigger arcs can lead to sustained arcing from one solar cell to another in the same or neighboring string. In this situation, the arc is fed by string photo-generated current and voltage. Based on plasma tank testing (Ref. 22), a sustained arc requires at least ~1-amp current and ~40-volt voltage levels (i.e., a power level > 40-watts) and proximate cell-to-cell spacing (i.e., 1.0×10^{-3} m). If they do occur, sustained arcs can be of long duration and high energy so that solar cells can become damaged, degraded or totally incapacitated due to short-circuit or open-circuit failure modes. The possibility of sustained arcing on a SAW string is extremely remote. This is due to the fact that closely spaced cells (in an 8-cell submodule) will operate at a voltage difference, $\Delta V_{submodule}$, no greater than about 7-volts (8 × Voc cell cold = 8×0.83-volts = 6.6-volts). A 7-volt potential is insufficient to maintain a sustained arc. In addition, the SAW string is comprised of two adjacent panels with a maximum cold solar cell voltage difference, ΔV_{max}, of about Voc or 332-volts (Fig. 28). However, these solar cells at different voltages are separated by a distance of 7.6-cm across an insulating panel hinge line. Sustained arcing has not been observed in this voltage regime during ground tests with simulated low Earth orbit plasma and electrode spacings greater than about 1-cm (Ref. 23). Thus, sustained arcing on even a cold SAW string is very unlikely to occur.

For all cases of SAW string operating under full-moon, EMU helmet flood and VCL eclipse lighting conditions, the estimated string voltage and current levels are far less than trigger arc voltage thresholds and sustained arcing thresholds. In addition, if the ISS plasma contactor is properly functioning, the ISS structure (to which the SAW string negative end is grounded) will be maintained within 40-volts of plasma neutral regardless of SAW string voltage. Therefore, solar cell arcing on SAW strings with continuity and proper grounding is extremely unlikely.

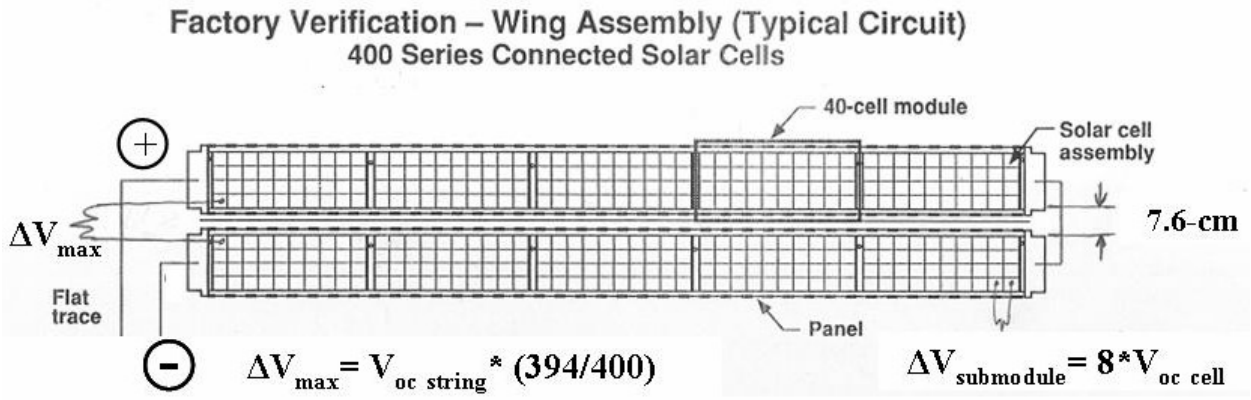

Figure 28.—Schematic electrical layout of a SAW string.

7.2 Power Connector Pin

During the SSU remove and replace eclipse EVA, connectors will be exposed to space plasma after cover removal or SSU demating. On the back of the SSU and on the beta gimbal platform are mating rectangular ORU connectors (Spec SSQ22680-001, -011, -007; made by G&H Technology) that are shown in Figure 29. There are also test port connectors (Part #LJT07RT21-35-5N and -5A) that are splice connections to SAW string power harness and located on the SAW mast canister (Fig. 30).

SSU power connectors and test port connectors are designed for nominal voltages above 160-volts without arcing. This voltage capability is far greater than the maximum steady state SAW voltage that can be generated under eclipse lighting scenarios (i.e., in the 50's of volts or less). Test port connectors and mating power connectors on the beta gimbal platform have sockets isolated by an insulating insert and grounded connector shells. The design features minimize the possibility of connector arcing. These features also minimize the risk of EVA crew inadvertent contact with an exposed, energized connector. From the standpoint of molten metal hazard, the eclipse lighting scenarios generate steady state SAW string power levels three orders of magnitude smaller than the threshold for connector pin molten metal hazard.

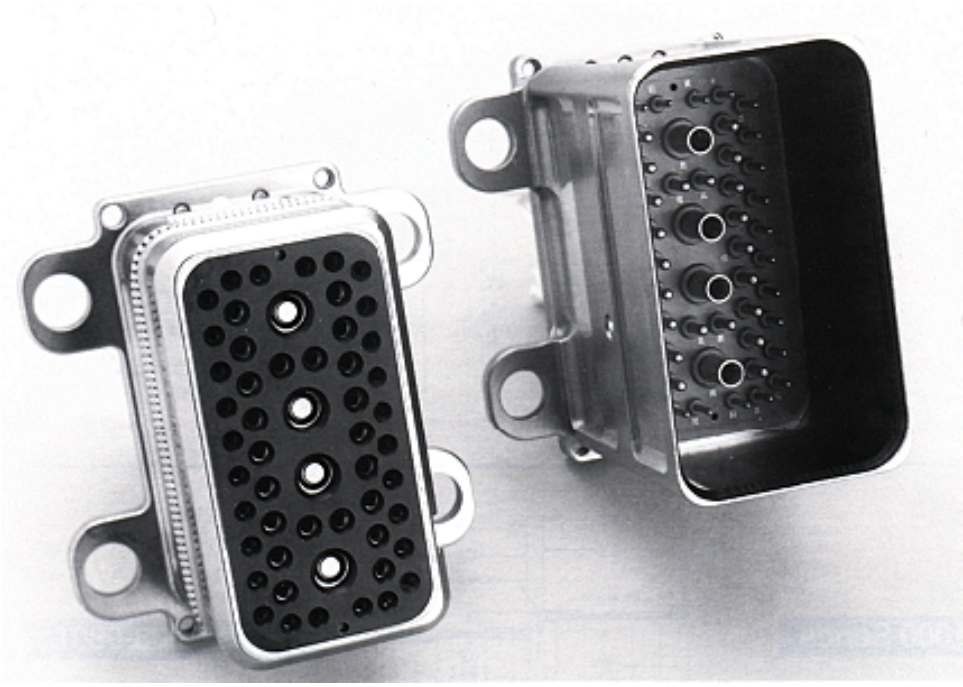

Figure 29.—SSU ORU power connectors.

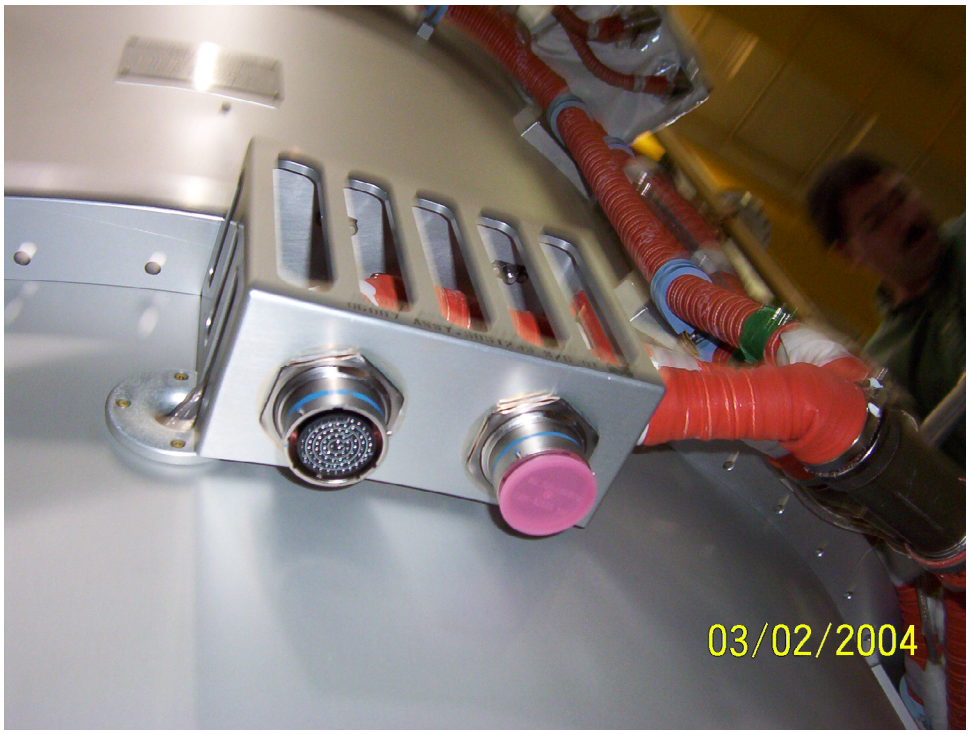

Figure 30.—Mast canister test port connectors.

This preliminary arcing assessment considered only steady state voltages and currents that could be generated by SAW strings under eclipse lighting conditions. This assessment *did not* consider transient current and voltages due to participating electrical circuit capacitance (particularly capacitance in the SSU input and output filters).

8.0 Conclusions/Recommendations

The following conclusions are based on the SAW string electrical hazard standards of: (1) shock hazards to EVA crew if current exceeds 0.001-amp and if voltage exceeds 32-volt DC and (2) connector pin molten metal hazard if current exceeds 3-amp per pin or exceeds 180-watts per pin. Based on this assessment of worst-case (greatest) SAW string steady state electrical performance under best-case (greatest) eclipse lighting conditions, there is no connector pin molten metal hazard. There is no EVA crew member shock hazard for cases of full moon illumination or EMU helmet lighting conditions or combined full moon plus EMU helmet lighting conditions. *EVA crew member electrical current and/or voltage hazards limits were exceeded for ISS-11A and post -15A VCL lighting cases*. Combining full moon plus EMU helmet lighting with VLC lighting only increased SAW string electrical performance slightly (~1 percent or less).

SAW string electrical performance under ISS-11A VCL lighting would likely drop below EVA electrical hazard limits under typical-case, VCL illumination conditions. This must be confirmed by repeating the performance assessment using more detailed and accurate SSU remove & replace EVA scenarios that include the exact geometry of the SAWs and VCLs

(gimbal position and pan angles). The SAW string voltage will likely not drop below EVA electrical hazards limits under typical-case, ISS post-15A VCL illumination conditions if the VCL is directed at the SAW. This conclusion is based on VCL-panel data and prior 1-Sun angle-of-incidence test data. Even if edge-on to the VCL beam, an in-board SAW string on a post-15A ISS would have a Voc of about 37-volts (or about 16 percent higher than the 32-volt hazard threshold value). Therefore, operational solutions to eliminate SAW string voltage hazard from VCL illumination are required. Potential solutions include: (1) power down the VCL at issue or (2) select a VCL pan angle to point the beam away from the SAW of interest (so that <50 percent of string solar cells are illuminated).

Based on a preliminary assessment, there is minimal risk of electrostatic discharge from or between SAW string solar cells under any eclipse lighting condition. Similarly, there is minimal risk of electrostatic discharge at SSU power connectors and test port connectors due to steady state SAW string current and voltage under any eclipse lighting condition. Connector discharge behavior from transient electrical circuit capacitive effects was not assessed.

The authors recommend that the SAW string electrical performance assessment under VCL eclipse lighting conditions be repeated once detailed and accurate SSU remove & replace EVA procedures have been developed. The procedures must include the exact geometry of the SAWs and VCLs including SAW alpha and beta gimbal positions and VCL positions and pan angles. The product of this assessment would be SAW gimbal and/or VCL pan angle keep-out-zones (KOZs) to decrease SAW current and voltage levels generated as a result of VCL lighting to safe levels. The authors also recommend that the EVA crew member electrical hazard thresholds be confirmed as-is or revised to the best possible values to maximize crew safety.

The uncertainty level in this proposed detailed KOZ assessment could be reduced with additional VCL lighting data. Specifically, measure the total wavelength-integrated light intensity in W/m^2 to correlate with the intensity data given in lumens. Measure the VCL beam intensity around the beam limb (beyond the 23-ft by 23-ft grid) out to a radial position where the light intensity drops to a level at or below 10 percent of the intensity in the beam center. And lastly, measure VCL primary beam flux intensity distribution on test planes at 3 distances from the VCL; perhaps at distances of 10, 15, and 20-m.

9.0 References

1. G. Landis, “Review of Solar Cell Temperature Coefficients for Space,” Proc. XIII Space Photovoltaic Research and Technology Conference, NASA CP–3278, NASA Lewis Research Center, June 1994, 385–400.
2. Scheiman, David A., et al., “Low Intensity, Low Temperature (LILT) Measurements on New Photovoltaic Structures,” 30th Intersociety Energy Conversion Engineering Conference, paper 95353, Aug 1995.
3. Stella, P.M. and Ctory, G.T. , “Solar Cell Design For Avoiding LILT Degradation,” Proceedings of the 19th IEEE Photovoltaic Specialists Conference, New Orleans, LA, May 4–8, 1987, pp. 636–640.
4. Stella, Paul M., et al., “PV Technology For Low Intensity, Low Temperature Applications,” Proceedings of the 1st IEEE World Conference on Photovoltaic Energy Conversion, Hawaii, December 5–9, 1994, pp. 2082–2087.

5. Strobl, G. et al., "Development of Advanced Si and GaAs Solar Cells for Interplanetary Missions," 14th Space Photovoltaic Research and Technology 1995, October 1, 1995, pp. 10–20.
6. Richards, N., and Greene, Jay H., "Interpretations of NSTS/ISS Payload Safety Requirements (Previously Titled NSTS 18798A)," NSTS/ISS 18798 Revision B, NASA JSC, September 1997.
7. Anonymous, "NSTS/ISS 18798 Revision B, September 1997, JSC Letter MA2-99-170, Crew Mating/Demating of Powered Connectors," Training Presentation/Quiz.
8. Nahra, Henry K., et al., "The Space Station Photovoltaic Panels Plasma Interaction Test Program: Test Plan and Results," paper no. AIAA–90–0722, 28th Aerospace Sciences Meeting, Reno, NV, January 8–11, 1990.
9. Kaufman, Bradford A., Chrulski, Daniel, and Myers, Roger M., "Photovoltaic Plasma Interaction Test II," NASA TP–3635, 1996.
10. Email, From "MOHR, EDWARD J. (JSC-XA) (NASA)" edward.j.mohr@nasa.gov, To: "Levy, Robert K" <robert.k.levy@boeing.com>, et al., Subject: RE: SSU Developments, Date: Mon, 22 Mar 2004 07:54:09 -0600. (Personal communication, E.J. Mohr, NASA Johnson Space Center, Houston, Texas 77058, May 2004.)
11. Spectrolab Inc., "Silicon K6700B Wrapthru Solar Cells – product data sheet," http://www.spectrolab.com/prd/prd.htm, November 2004.
12. Kerslake, Thomas W., Hoffman, David J., and Scheiman, David A., "Pre-Flight Dark Forward Electrical Testing of the Mir Cooperative Solar Array," 32nd Intersociety Energy Conversion Engineering Conference, Honolulu, Hawaii, July 27—August 1, 1997. (see also NASA TM–107496).
13. Kerslake, Thomas W., and Hoffman, David J., "Performance of the Mir Cooperative Solar Array After 2.5 Years in Orbit," 34th Intersociety Energy Conversion Engineering Conference, SAE 99–01–2632, Vancouver, British Columbia, Canada, August 1–5, 1999. (see also NASA/TM—1999-209287).
14. Dobber, Marcel R., "GOME Moon Measurements, Including Instrument Characterisation and Moon Albedo," The 3rd ERS Symposium Space at the service of our Environment, March 14–21, 1997, pp. 743–747.
15. Spectrolab Mark 2 X-25 simulator, ILS_X-25.pdf product data sheet from http://www.spectrolab.com, August 2003.
16. Jenkins, Phillip, et al., "Design and Performance of a Triple Source Air Mass Zero Solar Simulator," 18th Space Photovoltaic Research and Technology Conference, Ohio Aerospace Institute, Cleveland, OH, September 16–18, 2003.
17. McDonnell Douglas Specification Control Drawing 1F01194 "Luminaire, Camera, Video," NAS15–10000, Approved April 10, 1992.
18. Brinker, D.J., Scheiman, D.A., and Jenkins, P., "Calibration of Space Solar Cells Using High Altitude Aircraft" 2nd World Conference on Photovoltaic Solar Energy Conversion - PVSC 26, Vienna, Austria, VA6.15, July 6–10, 1998, p. 3654.
19. Delleur, Ann M., Kerslake, Thomas W., and Scheiman, David A., "Analysis of Direct Solar Illumination on the Backside of Space Station Solar Cells," 34th Intersociety Energy Conversion Engineering Conference, SAE 99–01–2431, Vancouver, British Columbia, Canada, August 1–5, 1999. (See also NASA/TM—1999-209377).
20. Bordina, N.M., Zayavlin, V.R., Kagan, M.B. and Letin, V.A., "Solar Batteries With Bifacial Sensitivity," Geliotekhnika, Vol. 28, No. 1, 1992, pp. 39–47.

21. Heard, John W., "Plasma Interaction with International Space Station High Voltage Solar Arrays," Research Reports: 2001 NASA/ASEE Summer Faculty Fellowship Program, NASA/CR—2002-211840, July 2002, p. XXI-1 - XXI-5.
22. Schneider, T., et al., "Plasma Interactions With High Voltage Solar Arrays For A Direct-Drive Hall Effect Thruster System," paper no. AIAA–2003–5017, 39th AIAA/ASME/SAE/ASEE Joint Propulsion Conference and Exhibit, Huntsville, AL, July 20–23, 2003.
23. Personal communication, Dr. Boris Vayner, NASA Glenn Research Center, Cleveland, Ohio 44135, March 2004.

REPORT DOCUMENTATION PAGE

Form Approved
OMB No. 0704-0188

1. AGENCY USE ONLY (*Leave blank*)	2. REPORT DATE	3. REPORT TYPE AND DATES COVERED
	October 2005	Technical Memorandum

4. TITLE AND SUBTITLE

Off-Nominal Performance of the International Space Station Solar Array Wings Under Orbital Eclipse Lighting Scenarios

5. FUNDING NUMBERS

WBS–22–336–31–01–AB

6. AUTHOR(S)

Thomas W. Kerslake and David A. Scheiman

7. PERFORMING ORGANIZATION NAME(S) AND ADDRESS(ES)

National Aeronautics and Space Administration
John H. Glenn Research Center at Lewis Field
Cleveland, Ohio 44135–3191

8. PERFORMING ORGANIZATION REPORT NUMBER

E–15311

9. SPONSORING/MONITORING AGENCY NAME(S) AND ADDRESS(ES)

National Aeronautics and Space Administration
Washington, DC 20546–0001

10. SPONSORING/MONITORING AGENCY REPORT NUMBER

NASA TM—2005–213988
AIAA–2005–5671

11. SUPPLEMENTARY NOTES

Prepared for the Third International Energy Conversion Engineering Conference sponsored by the American Institute of Aeronautics and Astronautics, San Francisco, California, August 15–18, 2005. Thomas W. Kerslake, NASA Glenn Research Center; and David A. Scheiman, Ohio Aerospace Institute, 22800 Cedar Point Road, Brook Park, Ohio 44142. Responsible person, Thomas W. Kerslake, organization code PBP, 216–433–5373.

12a. DISTRIBUTION/AVAILABILITY STATEMENT

Unclassified - Unlimited
Subject Categories: 18 and 20

Available electronically at http://gltrs.grc.nasa.gov

This publication is available from the NASA Center for AeroSpace Information, 301–621–0390.

12b. DISTRIBUTION CODE

13. ABSTRACT ***(Maximum 200 words)***

This paper documents testing and analyses to quantify International Space Station (ISS) Solar Array Wing (SAW) string electrical performance under highly off-nominal, low-temperature-low-intensity (LILT) operating conditions with non-solar light sources. This work is relevant for assessing feasibility and risks associated with a Sequential Shunt Unit (SSU) remove and replace (R&R) Extravehicular Activity (EVA). During eclipse, SAW strings can be energized by moonlight, EVA suit helmet lights or video camera lights. To quantify SAW performance under these off-nominal conditions, solar cell performance testing was performed using full moon, solar simulator and Video Camera Luminaire (VCL) light sources. Test conditions included 25 to –110 °C temperatures and 1- to 0.0001-Sun illumination intensities. Electrical performance data and calculated eclipse lighting intensities were combined to predict SAW current-voltage output for comparison with electrical hazard thresholds. Worst case predictions show there is no connector pin molten metal hazard but crew shock hazard limits are exceeded due to VCL illumination. Assessment uncertainties and limitations are discussed along with operational solutions to mitigate SAW electrical hazards from VCL illumination. Results from a preliminary assessment of SAW arcing are also discussed. The authors recommend further analyses once SSU, R&R, and EVA procedures are better defined.

14. SUBJECT TERMS

Electric power; Solar arrays; International Space Station; Tests; Solar cells; Low temperature tests

15. NUMBER OF PAGES

55

16. PRICE CODE

17. SECURITY CLASSIFICATION OF REPORT	18. SECURITY CLASSIFICATION OF THIS PAGE	19. SECURITY CLASSIFICATION OF ABSTRACT	20. LIMITATION OF ABSTRACT
Unclassified	Unclassified	Unclassified	